

**Altered gene expression by sedaxane increases PSII efficiency, photosynthesis and growth and improves tolerance to drought in wheat seedlings**

Olubukola O. Ajigboye<sup>a</sup>, Chungui Lu<sup>a1</sup>, Erik H. Murchie<sup>a</sup>, Christian Schlatter<sup>b</sup>, Gina Swart<sup>b</sup> and Rumiana V. Ray<sup>a\*</sup>

<sup>a</sup>School of Biosciences, University of Nottingham, Sutton Bonington, Loughborough, Leicestershire LE12 5RD

<sup>b</sup>Syngenta Crop Protection, Schwarzwaldallee 215, 4058 Basel Switzerland

**\* Corresponding author;** email [Rumiana.Ray@nottingham.ac.uk](mailto:Rumiana.Ray@nottingham.ac.uk)

**<sup>1</sup>Present address:** School of Animal Rural & Environmental Sciences, Nottingham Trent University, Brackenhurst Campus, Southwell, Nottinghamshire NG25 0QF

**KEYWORDS**

Sedaxane, Photosystem II, Gene expression, Drought, Wheat

**ABSTRACT**

Succinate dehydrogenase inhibitor (SDHI) fungicides have been shown to increase PSII efficiency and photosynthesis under drought stress in the absence of disease to enhance the biomass and yield of winter wheat. However, the molecular mechanism of improved photosynthetic efficiency observed in SDHI-treated wheat has not been previously elucidated. Here we used a combination of chlorophyll fluorescence, gas exchange and gene expression analysis, to aid our understanding of the basis of the physiological responses of wheat seedlings under drought conditions to sedaxane, a novel SDHI seed treatment. We show that sedaxane increased the efficiency of PSII photochemistry, reduced non-photochemical quenching and improved the photosynthesis and biomass in wheat correlating with systemic changes in the expression of genes involved in defense, chlorophyll synthesis and cell wall modification. We applied a coexpression network-based approach using differentially expressed genes of leaves, roots and pregerminated seeds from our wheat array datasets to identify the most important hub genes, with top ranked correlation (higher gene association

30 value and z-score) involved in cell wall expansion and strengthening, wax and pigment  
31 biosynthesis and defense. The results indicate that sedaxane confers tolerant responses of  
32 wheat plants grown under drought conditions by redirecting metabolites from defense/stress  
33 responses towards growth and adaptive development.

34

## 35 1. INTRODUCTION

36 Drought is considered the most important environmental factor limiting growth, plant  
37 metabolism and crop productivity worldwide [1]. Photosystem II (PSII) is the most important  
38 protein-pigment complex in the chloroplast that is also most vulnerable to drought stress [2].  
39 Under severe drought, often associated with elevated leaf temperatures and light levels, the  
40 limitation in CO<sub>2</sub> uptake coupled with an increased excitation energy in PSII and absorption of  
41 light energy in excess of that required for photosynthesis causes an imbalance between PSII  
42 activity and the Calvin cycle. This can result in photodamage to the PSII oxygen-evolving  
43 complex [3],[4], disruption of D1 protein involved in PSII repair, and subsequent inactivation  
44 of PSII reaction centers [5]. To protect the chloroplast, plants have evolved photoprotective  
45 responses to rapidly dissipate excess excitation energy as heat. Thermal dissipation of light  
46 energy by the light-harvesting antenna complex of PSII, measured as non-photochemical  
47 quenching (NPQ), is one of the most important rapidly activated regulatory mechanisms in  
48 plants to avoid irreversible photodamage [6]. NPQ is triggered by the light-driven build-up of a  
49 transthylakoid proton gradient ( $\Delta pH$ ). The acidification of the thylakoid lumen results in the  
50 protonation of PSII LHC antenna regulatory proteins such as PsbS [7] and the de-epoxidation  
51 of xanthophyll cycle pigment violaxanthin into zeaxanthin [6],[8]. Whilst reducing the likelihood  
52 of photoinhibitory damage, NPQ momentarily reduces the quantum yield of CO<sub>2</sub> assimilation.  
53 Although this is a highly regulated process that reduces the likelihood of oxidative stress,  
54 photoprotection can also be considered to compete with photochemistry for absorbed energy  
55 [9]. Plant under drought stress typically show rapid increase in NPQ with increasing  
56 illumination coupled with decreased capacity for photosynthesis [10]

57 Fungicides of the class of succinate dehydrogenase complex II inhibitors (SDHIs) however  
58 have been recently shown to significantly increase the efficiency of PSII photochemistry  
59 ( $F_v'/F_m'$ ) of wheat grown under drought stress, in the absence of disease, resulting in  
60 improved photosynthesis and yield under controlled and field conditions [11],[12]. Changes in  
61  $F_v'/F_m'$  were detected in plants grown in field and under controlled environments within 4 h of

fungicide application.  $F_v/F_m'$  is indicative of changes in PSII operating efficiency attributed to thermal dissipation, which correlates in a non-linear fashion with decreasing thermal dissipation of excitation energy in the light harvesting complexes of PSII, estimated as non-photochemical quenching or NPQ [2]. Thus it is likely that increased PSII efficiency (indicated as  $F_v/F_m'$ ) and improved photosynthesis in SDHIs treated plants may be accompanied by reductions in NPQ. It is currently unclear how this effect on PSII and photosynthesis occurs: the succinate dehydrogenase (SDH; succinate: ubiquinone oxidoreductase) complex plays a central role in mitochondrial metabolism, catalyzing the oxidation of succinate to fumarate and the reduction of ubiquinone to ubiquinol, thereby linking the tricarboxylic acid (TCA) cycle and the electron transport system. In fungi, SDHIs specifically block the ubiquinone-binding sites in the mitochondrial complex to disrupt cellular respiration and energy generation [13]. Although the mode of action of these compounds on fungal metabolism is well understood, the effects on plant metabolism and the molecular basis of the observed physiological responses to drought stress in SDHI treated plants remain unknown.

In this work, we investigated the effects of sedaxane, a novel SDHI fungicide, belonging to the chemical class of pyrazole-carboxamides, formulated to use on crops as seed treatment to provide local and systemic protection of the seed, seedling and roots against soil-borne plant pathogenic fungi [14]. The active ingredient is typically absorbed from the soil matrix by the developing plant roots and translocated within the seedling with systemic activity of 4-6 weeks following seed germination. We combined chlorophyll fluorescence with gas exchange measurements to measure PSII efficiency and photosynthesis of plants grown from sedaxane treated seeds. Our aim was to better understand the molecular mechanism for improved photosynthetic efficiency, growth and biomass of SDHI-treated wheat grown under drought stress in the absence of disease using transcriptomics approach. The objective of this paper was to address the following questions. (1) Can sedaxane improve photosynthesis and PSII efficiency and is this characterized by low NPQ under drought? (2) Are these phenotypic effects associated with transcriptomic changes? (3) Do these changes lead to modifications

in physiological processes with sedaxane applied as seed treatment? We integrated whole plant physiological responses with changes in global gene expression in leaf tissues to obtain more comprehensive understanding of the regulatory genetic mechanisms underlying the physiological responses of SDHI treated plants under drought stress.

The focus of our investigation was the leaf as the main photosynthetic organ maximizing carbon assimilation [15] and a major target for improving photosynthetic efficiency. However, the root and pregerminated seed tissues were included in the gene co-expression and gene network analysis to aid our understanding of the interactions regulating plant responses to sedaxane under drought conditions because of translocation and systemic activity of sedaxane into developing tissues following seed germination.

## **2. MATERIALS AND METHODS**

### **2.1. Plant Growth Conditions and Experimental Design**

Two experiments were carried out. Experiment 1 was used to measure sedaxane treated plants for photosystem II efficiency and photosynthesis using detailed chlorophyll fluorescence and gas exchange analysis. Experiment 2 was designed for transcriptomics analysis. Plant tissues were collected for RNA isolation as soon as changes in PSII efficiency were confirmed on indicator plants using portable fluorometer (Fluorpen FP100, Photon System Instruments, Czech. Republic).

Winter wheat seed (cv. Gallant) were treated with Sedaxane at 10g a.i./100kg seed (Syngenta Crop Protection UK, Cambridge) or left untreated. Untreated and treated seeds were initially tested on potato dextrose agar medium (PDA) for any fungal or bacterial infection to ensure that only healthy seeds were used in all experiments [16]. Plants were grown in a walk-in growth chamber at the University of Nottingham with controlled temperature and light intensity of 15°C and 300  $\mu\text{mol m}^{-2}\text{s}^{-1}$ , respectively. Photoperiod was maintained at 8 h light/16 h dark throughout the course of the experiment. Seeds were pre - germinated on water moistened filter paper for 2 d prior to planting into 9cm, 0.36L pots filled with either compost (John Innes 2, experiment 1) or  $\gamma$ -radiated loamy sand soil (experiment 2) prepared as described by Sturrock et al. [17]. The amount of water in soil available to the plants at field capacity was determined as described by Ajigboye et al. [11]. Water was initially supplied to 60% of available water at full field capacity ( $\text{AW}_{\text{FC}}$ ) and maintained at either 10% or 90%  $\text{AW}_{\text{FC}}$ .

Experiment 1 was designed as randomized block with two factors, fungicide treatment (sedaxane treated or untreated) and soil moisture (90% or 10% available water at full field capacity). There were seven replications of each treatment. Plants were divided into two groups; “drought-stressed” and “non-stressed”, each group with equal number of treated and untreated seedlings. Water was withheld from the drought-stressed plants to attain 10% available water at full field capacity ( $\text{AW}_{\text{FC}}$ ) by 8 days after germination (DAG) while non-

stressed plants were supplied with sufficient water to attain 90%  $AW_{FC}$  at 3 DAG and maintained at the same available water until the end of the experiment. Experiment 2 was designed as randomized block with two treatments, sedaxane or untreated and consisted of 22 replicates, seven of which were considered as indicator plants while samples for RNA isolation were collected from the remaining 15 replicates. All plants were maintained at 10%  $AW_{FC}$  from 5 DAG.

## **2.2. Experiment 1: Photosynthetic Efficiency and Growth Analysis**

The polyphasic rise in chlorophyll a fluorescence (OJIP) transient was measured using portable fluorometer (Fluorpen FP100, Photon System Instruments, Czech Republic) between 12-2pm daily from 9 to 11 DAG. Leaves were not dark adapted prior to obtaining measurements. Therefore, we describe minimal and maximal fluorescence as  $F_o'$  and  $F_m'$ , respectively. OJIP transient was induced by strong light pulse of  $3000 \mu\text{mol m}^{-2}\text{s}^{-1}$ . Data extracted along the recorded transient include fluorescence intensity at 50  $\mu\text{s}$ , considered to be minimal fluorescence  $F_o'$ , fluorescence intensity at J-step (2 ms), i-step (60 ms) and at the peak of the transient P ( $=F_m'$ ).  $F_v'/F_m'$  was computed as  $[(F_m' - F_o')/F_m']$ . Biophysical parameters involving energy fluxes per reaction centers were automatically computed from the transient curve using the JIP test as defined by Strasser et al [18]. Photosystem II quantum yield was measured independently of the OJIP transient. Measuring light of  $900 \mu\text{mol m}^{-2}\text{s}^{-1}$ , was applied to acquire minimal fluorescence  $F_o'$  followed by a saturating light pulse of  $3000 \mu\text{mol m}^{-2}\text{s}^{-1}$  to measure  $F_m'$ . QY is considered equivalent to  $[F_v'/F_m']$  in light adapted plants. All measurements were made on the youngest fully expanded leaf on each plant.

At 12 DAG, light response of gas exchange and chlorophyll fluorescence were quantified simultaneously using an infra-red gas analyzer, LI6400XT, equipped with leaf chamber pulse-amplitude modulated fluorometer LI6400-40 (LI-COR, Lincoln, NE, USA). Leaves were dark adapted in the growth chamber for 60 min prior to measurement by wrapping sections

of the leaf in low-weight silver aluminium foil. The dark-adapted leaves were placed in the chamber, they were left for 5 min in the dark before  $F_0$  was measured and then a saturating pulse applied to measure  $F_m$ . At this point the actinic light was applied. In the light-adapted state  $F_m'$  was measured by applying a saturating pulse of  $7000 \mu\text{mol m}^{-2} \text{s}^{-1}$  (for 0.8 s).  $F_0'$  was measured by switching off the actinic for 2 s after the saturating pulse and applying far-red (FR) light. A series of illumination at PAR values was started at 0 and shifting to 2000, waiting for 3 min at each light intensity before measurement. Fluorescence and gas exchange parameters were calculated directly from the Licor software ([https://www.licor.com/env/products/photosynthesis/LI-6400XT/software\\_downloads.html](https://www.licor.com/env/products/photosynthesis/LI-6400XT/software_downloads.html)). Measurements were made under constant leaf temperature of  $18^\circ\text{C}$ ,  $\text{CO}_2$  concentration of  $400 \mu\text{l L}^{-1}$ , relative humidity 50- 55%, gas flow rate  $500 \mu\text{mol air s}^{-1}$  and photosynthetic photon flux density (PPFD) of  $1000 \mu\text{mol m}^{-2} \text{s}^{-1}$ .

Plant height was measured from the base of the plant to the tip of the longest leaf. Plants were harvested 32 days after transplanting, fresh weights were measured before plants were oven-dried at  $80^\circ\text{C}$  for 72 h to a constant weight. Dry weight was defined as dry weight/fresh weight. Percentage water content was defined as (fresh weight – dry weight)/fresh weight.

## **2.3. Experiment 2: Gene Expression Analysis**

### **2.3.1. Sampling**

Chlorophyll (Chl) a fluorescence transient (OJIP) induced as described in experiment 1, was measured daily on the fully expanded leaf on the main shoot of plants considered as indicator plants from 5 DAG. OJIP was induced as described in experiment 1. As soon as significant differences ( $P < 0.05$ ) in PSII efficiency ( $F_v'/F_m'$ ) between treatments were detected in the indicator plants at 9 DAG, leaf and root samples were collected individually from the remaining 15 replicates for RNA extraction.

### **2.3.2. RNA Extraction**



Harvested tissues were immediately frozen in liquid nitrogen and stored at  $-80^{\circ}\text{C}$  prior to processing. Total RNA from leaf and roots of sampled plants as well as pre-germinated seeds (2 d) was extracted from 100mg tissue. Frozen tissues were homogenized in TRIzol using a FastPrep-24 (MP BIO) and lysing matrix D. Extracted RNA was then purified (RNeasy Mini Kit, Qiagen). The extracted RNA was quantified with a NanoDrop ND-2000 UN-VIS spectrophotometer (Thermo Scientific) and the integrity checked by fragment length on 2% agarose gel electrophoresis.

### **2.3.3. Microarray Experiments**

RNA from 3-5 individual plants was combined into one sample per treatment and replicate. Eighteen arrays were used in total, representing two treatments, three tissue types and three replicates. Hybridization of biotin-labelled RNA to Affymetrix Wheat GeneChip arrays and array scanning were carried out at the University of Nottingham Affymetrix Microarray service according to the manufacturer's instructions ([www.affymetrix.com/support/technical/manual/expression.manual.affx](http://www.affymetrix.com/support/technical/manual/expression.manual.affx)). Normalization and analysis of differential expression was carried out using GeneSpring GX13 (Agilent Technologies). Baseline preprocessing and normalization were carried out using the Robust Multiarray Average summarization algorithm (RMA), as described by Irizarry et al. [19]. Tissues from the leaf root and pre-germinated seed were examined separately. A one-way ANOVA with Benjamini Hochberg FDR multiple test correction was applied in order to select genes that reveal significant changes ( $P < 0.05$ ) in their expression. All treatments for the tissues were compared with the control experiment of corresponding tissue. A cutoff value of 1.5-fold change was adopted to discriminate expression of genes that were differentially expressed in response to sedaxane treatment.

### **2.3.4. Gene Ontology Enrichment and Functional Pathway Analysis**

To categorize differentially expressed genes based on their biological functions, list of genes identified by microarray analysis ( $\geq 1.5$ -fold change) were submitted to MapMan for analysis

[20]. Transcripts were assigned into functional categories (or bins) of metabolism and cell function. The Wilcoxon Rank Sum test corrected with Benjamini Hochberg FDR multiple test was used to identify differentially regulated bins. Gene ontology enrichment of the gene lists was carried out using the Parametric Analysis of Gene Set Enrichment (PAGE) in the agriGO toolkit (<http://bioinfo.cau.edu.cn/agriGO/analysis.php>) [21]. Benjamini-Hochberg multi-test adjustment method for the P-value was selected. P-value of 0.05 and false discovery rate (FDR) <0.05 was used as a cutoff to select significantly enriched GO terms.

### **2.3.5. Genome-scale gene network analysis**

A web-based Genome-scale gene network method was used. RMA normalized microarray data were uploaded to the DeGNServer <http://plantgrn.noble.org/DeGNServer/Analysis.jsp>. Networks with reduced edge densities were generated on the basis of co-expression (cut-off >0.8) and Context Likelihood or Relatedness (CLR, at a cut-off of >3.6). The constructed network and sub network were uploaded into Cytoscape [22] for visualization. The ranked genes and common subgraphs of key differentially expressed genes were produced in both the DEGNserver and Cytoscape. All the differential expressed genes of each set were selected to build a sub-expression profile unit, and were implemented for correlation analysis by value-based co-expression network method (gene association value). Considering the computational speed and empirical accuracy comparison, z-scores value based co-expression method and Spearman's rank correlation estimation method were applied in our analysis.

### **2.3.6. qRT-PCR**

To validate the microarray experiment, RNA from microarray as well as from an independent experiment was used for qRT-PCR. DNase treated RNA were from the microarray experiment and from plants of a different seed lot grown under the same controlled environmental conditions described earlier. qRT-PCR was performed for six genes from the gene network analysis (Table S1). CFX96 (Bio-Rad, UK) was used for qPCR with iTaq™ Universal SYBR® Green one-step kit (Bio-Rad). Reactions consisted of 2 µL of 20 ng of total

RNA, 0.012 µL of 300nM forward and reverse primers, 5 µL of iTaq™ Universal SYBR® Green reaction mix (2x), 0.125 µL of iScript reverse transcriptase and 2.8 µL of nuclease-free water for a final reaction volume of 10 µL. Reactions were under the following conditions: 50°C for 10 min, 95°C for 1 min, then 40 cycles of 10 s at 95°C for denaturation and 15 s at 60°C for annealing, extension and plate read. At the end of each reaction, dissociation curve was performed from 65°C–95°C in 0.5°C increments for 0.05 s, which confirmed a single peak for each set of primers. No-template controls were included for each primer set per run to confirm the absence of contamination and primer dimer. No-template control consistently recorded no signal or were significantly suppressed, with signals recorded after 10 or more cycle threshold above the target signal. No-reverse transcription controls were run for each RNA sample to confirm the absence of genomic DNA contamination. The PCR reactions were performed in triplicates for each gene being validated. The quantification cycle (Cq) for each type of PCR product were determined for all samples using Bio-Rad CFX Manager 3.1 (Bio-Rad, UK). All Cq values were normalized to two reference genes, Ubiquitin-conjugating enzyme and Cell division control protein, AAA-superfamily of ATPases [23].

#### **2.4. Statistical analysis**

Analysis of variance (ANOVA) of chlorophyll fluorescence, and gas exchange parameters, and biomass were performed with Genstat 16<sup>th</sup> Edition (VSN International). Treatments were considered significantly different at Least Significant Difference (LSD) of 5% ( $P \leq 0.05$ ).

### 3. RESULTS

#### 3.1. Sedaxane Improves Wheat Photosynthetic Efficiency under Drought Stress

##### Conditions

We first used fast induction chlorophyll fluorescence (OJIP) transient to rapidly quantify changes in chlorophyll fluorescence parameters measured on plants grown at 10% (drought-stressed) and 90% (non-stressed) available water at field capacity ( $AW_{FC}$ ). This technique allowed us to monitor the efficiency of photosystem (PS) II of the youngest fully expanded leaf of the primary plant tiller over a 3 d period. Across both treatments, there were no interactions between sedaxane and water regime. The main effect of sedaxane treatment from 9 to 11 DAG on efficiency of PSII photochemistry ( $F_v/F_m'$ ), quantum yield (QY) and dissipated energy flux ( $Dlo/RC$ ) are shown in Fig. 1. The efficiency of PSII photochemistry ( $F_v/F_m'$ ) increased with sedaxane treatment from 9 DAG compared with the untreated control, with the highest increase ( $P<0.05$ ) observed at 11 DAG (Fig. 1A). A similar trend was observed for QY (Fig. 1B). Dissipated energy flux ( $Dlo/RC$ ) per PSII active reaction center was lower in plants grown from sedaxane treated seeds from 9 DAG and remained lower (8%  $P<0.05$ ) than the untreated plants 11 DAG (Fig. 1C). The above results showed that sedaxane had a significant impact on PSII photochemistry. Therefore, we quantified the effect of sedaxane on the photosynthetic performance of drought-stressed and non-stressed plants through simultaneous measurement of leaf chlorophyll fluorescence (CF) and gas exchange parameters 12 DAG under a range of incident light fluxes. Drought stress (10%  $AW_{FC}$ ) at 12 DAG resulted in a significant decrease in  $qP$  compared to non-stressed plants (90%  $AW_{FC}$ ) at higher light intensities above  $750 \mu\text{mol m}^{-2}\text{s}^{-1}$  (Fig. 2). The rate of stomatal conductance under drought stress declined by almost 17% ( $P<0.05$ ) at each light intensity compared to the non-stressed control (Fig. S1A). A similar trend was observed for the rate of leaf transpiration although the effect was significant ( $P<0.05$ ) under higher light intensities between  $1200$  to  $2000 \mu\text{mol m}^{-2}\text{s}^{-1}$  (Fig. S1B). Sedaxane-treated plants under both water availability regimes had 8% lower NPQ compared to untreated ( $P<0.05$ ) at high light intensities above  $1000 \mu\text{mol m}^{-2}\text{s}^{-1}$  (Fig.

3A). Generally, under the range of incident light fluxes, the rate of photosynthesis was 10% lower in drought-stressed plants than in non-stressed control. However, interactions between fungicide and  $AW_{FC}$  treatment showed that photosynthesis was 8% higher in sedaxane-treated plants grown under drought stress compared to untreated control ( $P < 0.05$ ; Fig. 3B).

At 12 DAG no further interactions were detected between treatments and the main effects of sedaxane or water availability on  $\Phi PSII$ ,  $F_v/F_m$  and  $F_v'/F_m'$  were not significant at LSD of 5% (data not shown).

Drought stress (10%  $AW_{FC}$ ) 36 DAG significantly reduced ( $P < 0.001$ ) tiller number by 78% (Table 1). There were significant interactions between seed treatment and  $AW_{FC}$  for plant height, total percentage water content and dry weight. Under drought stress, sedaxane increased plant height by 7% ( $P = 0.044$ ), reduced percentage water content ( $P = 0.027$ ) and increased dry weight by 37%, ( $P = 0.027$ ) compared to untreated control.

### 3.2. Microarray Analysis of Sedaxane-Responsive Genes

We showed that photosynthetic efficiency, photosynthesis and biomass increased in wheat plants from sedaxane treated seeds under drought conditions. To further understand the molecular basis of the observed physiological effects, we performed microarray analysis (Wheat GeneChips; Affymetrix) to determine gene expression. Genes were considered differentially regulated if their expression was significantly different from the untreated control ( $P < 0.05$ ). A total number of 4369 differentially regulated genes (adjusted  $P$  value of  $< 0.05$ ) were identified and we used a minimum cut-off of 1.5-fold change to identify genes that were robustly regulated by sedaxane (Table S2). The number of genes differentially regulated in response to sedaxane was 2200 in leaves (898 up-regulated and 1302 down-regulated), 514 in roots (237 up-regulated and 271 down-regulated) and 2066 in pre-germinated seeds (615 up-regulated and 1452 down-regulated). Comparison of the microarray data from all of the three tissues did not show any up-or down-regulated (Fig. 4), however less than 3% of the differentially expressed genes overlapped between any two tissues. Thus, most of the

regulated genes were tissue specific, indicating that pre-germinated seeds, leaves or root tissues respond to sedaxane by activating distinct sets of genes.

### **3.3. Functional Classification of Sedaxane Responsive Genes with Altered Expression**

MAPMAN software [20] was used to gain insight into the biological processes affected by sedaxane in each of the three tissues considered (Table 2 & 3;  $P < 0.05$ , Wilcoxon rank sum test in the MapMan tool). In the overview of cell function, analysis of differential gene expression in pregerminated seeds revealed a down-regulation of genes assigned to the categories DNA synthesis/chromatin structure encoding core histone H2A/H2B/H3/H4 domain containing protein and biotic stress generally encoding genes associated with disease resistance proteins, HEVEIN FAMILY PROTEIN, PATHOGENESIS-RELATED (PR) PROTEINS although majority of genes in the seeds were unassigned (Tables 2 & Table S3A). In roots, genes involved in biotic stress such as those encoding the PATHOGENESIS-RELATED PROTEINS and DEFENSIN-LIKE PROTEINS were down regulated. (Tables 2 & Table S3B). In the leaf, an overview of the transcriptional responses affecting genes coupled to cell function showed that genes connected to protein synthesis were up-regulated (Table 2 & Table S3C). These up-regulated genes encode the various sub units (30S, 40S, 50S and 60S) of ribosomal protein from the chloroplasts. In contrast, genes involved in hormone metabolism, signaling and biotic stress were generally down regulated (Table 2 & Table S3C). For example, in pathways involved in hormone metabolism, genes encoding jasmonate biosynthetic precursors, ethylene, auxin and abscisic acids were down-regulated. Similarly, most of the genes involved in signaling were down-regulated, including genes associated with CALCIUM SIGNALING, MITOGEN-ACTIVATED PROTEIN KINASES, LEUCINE RICH REPEAT PROTEIN KINASES FAMILY PROTEIN, although two genes associated with light signaling, encoding the EARLY LIGHT INDUCIBLE PROTEIN HV58, known to function against chlorophyll induced oxidative damage [24] were activated. In the stress category,

330 genes encoding defense related proteins and PR-proteins were generally down regulated  
331 except a dirigent-like protein which was upregulated (Table S3C).

332 In the overview of metabolism, enriched functional categories were detected in the leaf  
333 tissue only (Table 3). It is likely that several important transcripts which can exert significant  
334 changes in downstream gene expression to lead to a substantial biological effect were  
335 eliminated [25] in pregerminated seeds and roots due to our stringent criteria (fold change  
336  $\geq 1.5$ ). A closer look at the categories showed that genes involved in cell wall modification  
337 and tetrapyrrole synthesis categories were up-regulated (Table 3; Table S4). Upregulated  
338 genes related to cell wall modifications include the cell wall loosening EXPANSINS and cell  
339 wall-strengthening enzymes, XYLOGLUCAN ENDOTRANSGLYCOSYLASES (XTHs, Table  
340 S4). The set of genes involved in tetrapyrrole synthesis include those encoding chlorophyll  
341 precursors corresponding with the various steps in chlorophyll biosynthesis including  
342 DELTA-AMINOLEVULINIC ACID DEHYDRATASE, UROPORPHYRINOGEN  
343 DECARBOXYLASE, PROTOPORPHYRINOGEN IX OXIDASE, MG-PROTOPORPHYRIN IX  
344 and PROTOCHLOROPHYLLIDE REDUCTASE (Table S4).

345 We also explored changes in the abundance of transcripts from genes that mediate known  
346 biological processes and molecular function in the tissues using the Parametric Analysis of  
347 Gene Enrichment Analysis (PAGE) tool of agriGO [21]. Results showing the most enriched  
348 GO terms from these analyses are shown in Table 4 and 5. In pregerminated seeds, GO  
349 analysis identified molecular functions that were significantly enriched in up-regulated genes  
350 with the terms glutathione transferase activity and cofactor binding while down-regulated  
351 genes were enriched in DNA binding (Table 4). For biological processes, the most significantly  
352 enriched biological process was glutathione metabolic processes and nucleosome assembly  
353 for up-regulated and down regulated genes respectively (Table 4). There were no significantly  
354 enriched GO terms in the root. In the leaf, molecular functions with highly enriched GO terms  
355 for up-regulated genes were ribosomal RNA binding, GTP binding, structural constituent of  
356 ribosome and transferase activity while down-regulated genes enriched GO terms were

related to protein serine/threonine kinase activity and co-enzyme binding (Table 5). Enriched GO terms involved in biological processes for up-regulated genes were translation, ribosome biogenesis and chlorophyll metabolic process and significantly enriched categories for down-regulated genes were jasmonic acid biosynthetic process, defense response and response to other organisms (Table 5).

### **3.4. Co-expression and Gene Regulatory Network Analysis**

We analyzed co-expressed genes to identify the functional associations between sedaxane responsive genes that are part of the same biological process and may be under similar transcriptional control in all three different tissues. To identify genes associated with stress, we submitted the top 10 up/down-regulated genes as seed genes to exact sub-networks, the sub-networks were visualized with the DEGNServer and Cytoscape. The centrality to co-expression networks of hubs tend to be associated with essential roles in biological processes [26],[27]. Forty genes with the highest stress centrality followed by degree centrality (Fig. 5 and Table S5) were annotated using the PLEXdb annotation portal [28] and HarvEST (version 1.59). About 75% of the top genes were upregulated in the leaf, while only about 50% and 35% were upregulated in the root and pregerminated seeds respectively (Table S5). Among differentially induced genes associated with drought tolerance in the leaf and roots but down regulated in the pre-germinated seeds, were AQUAPORIN, CHOLINE DEHYDROGENASE, HESSIAN FLY RESPONSE GENE 1 PROTEIN, DIRIGENT LIKE PROTEIN (DIR), ZINC FINGER PROTEIN, 2-OXOGLUTARATE DEPENDENT OXYGENASE and DEHYDRIN. An exception to the group is the TYPE 1 NON SPECIFIC LIPID TRANSFER PROTEIN (nsLTPs), XYLOGLUCAN ENDOTRANSGLYCOSYLASES (XTHs) and WAX2 protein which were upregulated only in the leaf tissues. The GLYCINE-RICH PROTEIN (GRPs), MALTO-OLIGOSYLTREHALOSE TREHALOHYDROLASE, TRANSCRIPTIONAL REGULATOR LYSR, FRUCTAN EXOHYDROLASE and CYSTEINE SYNTHASE were among the down regulated genes in the leaf.



383 Six of the top genes with high stress and degree centrality (HFR1 and DIR, nsLTPs GRP –  
384 like, XTHs and an unknown gene *TaAffx.30098.1.S1\_at*) were selected for qRT-PCR analysis  
385 in the leaf tissue (Table S4 and Table S5). Excess RNA produced during microarray target  
386 preparation and from an independent experiment was used separately to provide template for  
387 qRT-PCR. The expression ratios produced by qRT-PCR and the microarray experiments were  
388 similar (Fig. 6), and except for the gene encoding GRPs, all the genes were confirmed as  
389 preferentially upregulated in leaf by both the microarray and qRT-PCR.

390

#### 4 DISCUSSION

Sedaxane applied as seed treatment induced significant increase in the efficiency of excitation energy capture by open PSII reaction centers ( $F_v'/F_m'$ ) in drought stressed plants. This is in agreement with previous studies showing similar effect exerted by another SDHI, isopyrasam, shown to enhance the photosynthetic efficiency of disease-free wheat plants under drought conditions [11]. Changes in  $F_v'/F_m'$  and  $Dlo/RC$  were used in this study as early indicators of modifications in PSII operating efficiencies attributed to thermal dissipation of excessive excitation energy in the light harvesting complexes of PSII, estimated as non-photochemical quenching or NPQ [29]. Under stress conditions, NPQ acts as a photoprotective mechanism by which PSII activity is down-regulated to prevent damage to PSII reaction centers. Consequently, decrease in NPQ accompanied with an increased rate of leaf photosynthesis in sedaxane treated plants under drought conditions suggests that sedaxane treatment led to preferential allocation of excitation energy into photochemical processes [30].

Sedaxane inhibits the succinate dehydrogenase (SDH) complex II in the fungal mitochondria and there is a possibility that similar effect may be exerted on the plant mitochondrial complex II although this hypothesis was not tested in the present study. Inhibition of SDH by partial reduction of SDH subunits has been reported previously to improve leaf photosynthesis and biomass by increasing stomatal conductance in tomato and Arabidopsis [31],[32]. Acevedo et al [33] recently reported that an SDH flavoprotein subunit (*SDH1-like*) transcript was upregulated in *Ilex paraguariensis* plants exposed to drought. This authors showed that increase in *SDH1-like* transcripts correlated with elevated ABA concentration. ABA accumulates in the guard cells of drought stressed plants to induce stomatal closure and conserve water. In the present study, genes encoding ABA were downregulated in sedaxane treated plants under drought. In addition, we detected interactions between sedaxane and  $AW_{FC}$  on stomatal conductance which were significant at 10% LSD (results not shown), suggesting that, treatment with sedaxane may have contributed to the

maintenance of stomata function under drought consistent with our observations of improved photosynthesis, increased biomass and reduced water content of sedaxane-treated wheat seedlings.

## **Transcriptome Response to Sedaxane in Plant Tissues**

In total, 4369 genes, around 7% of the genes present on the chip were found to be differentially expressed ( $P < 0.05$ ) in response to sedaxane seed treatment in all three tissues considered under drought conditions. About 50 % ( $\geq 1.5$ -fold change) of the differentially expressed genes (DEGs) were found in leaves and pregerminated seeds, while only 12% were found in the roots. When comparing DEGs in the three tissues collectively, no common DEGs were identified. However, about 3% DEGs overlapped in the leaf and pregerminated seed, and less than 1% in the leaf and root or the pregerminated seed and root tissues. Hence, distinct sets of genes were generally activated in individual tissues of drought stressed wheat seedlings in response to sedaxane. Our work thus offers the first comprehensive picture of transcriptional changes triggered by an SDHI, sedaxane, in distinct tissues of drought-stressed wheat plants associated with increased PSII efficiency and photosynthesis.

## **4.2. Cellular and Metabolic Responses to Sedaxane**

### **4.2.1 Pregerminated seeds and Roots**

No drought stress was introduced to the pregerminated seeds in this study; therefore, we consider gene differential expression in this tissue a direct effect of sedaxane seed treatment under non-stress conditions. Upregulated genes in response to sedaxane were significantly enriched in glutathione-s-transferase (GST) activity. GSTs are important proteins involved in efficient scavenging of plant toxins such as ROS, which accumulate as a consequence of increased oxidative stress [34] and thus maintain redox homeostasis in plant tissues [35]. Our results showed that the transcripts of these ROS scavenging proteins, GSTs accumulated during germination, to suggest a close association between sedaxane seed treatment protection of the plant (leaf) from oxidative stress under drought conditions.

Pathway analysis of all differentially expressed genes in the root showed that biotic stress was the only enriched pathway (Table 2). These genes encode pathogenesis-related proteins and defensin-like proteins, generally upregulated in response to pathogen attack which ultimately impede further pathogen invasion and enhance the capacity of the host to limit subsequent pathogen infection [36],[37]. Interestingly, many pathogenesis-related genes are also induced upon exposure of a plant to abiotic stress ensuring disease resistance [38]. In our study, all the genes in this category were downregulated suggesting treated roots were not exhibiting biotic stress related responses under drought possibly due to the protective properties of sedaxane.

## **4.2.2 Leaves**

### **4.2.2.1 Jasmonate Biosynthesis and Signaling**

Early plant responses to drought involve the adjustment of the levels of endogenous hormones to activate physiological pathways for adaptation, thereby modulating the expression of genes involved in processes relating to PSII, photosynthesis, cell modification, growth and development under abiotic stress conditions [39]-[41]. Hormone metabolism was one of the enriched pathways involved in key cellular functions in our study in particular genes involved in the jasmonate synthesis. This is substantiated by GO analysis showing enrichment for genes involved in jasmonic acid biosynthetic and metabolic processes (Table 5). JAs have been shown to play critical role in the early priming (preconditioning stage) to moderate drought in *Arabidopsis* (*Arabidopsis thaliana*), stimulating preparatory response for drought acclimation (for example stomatal closure and cell wall modification) [42]. Our datasets show that genes encoding the various derivatives of jasmonates among which are jasmonic acid and genes encoding enzymes involved in the biosynthetic pathway including allene oxide synthase, allene oxide cyclase; lipoxygenase and 12-oxophytodienoic reductase were downregulated. Under drought stress conditions in sedaxane treated plants, the JA-signaling genes involved in calcium signaling and mitogen-activated protein kinases were also downregulated. Calcium ion influx ( $\text{Ca}^{2+}$ ) and mitogen-activated protein kinases are key

components of JA signal transduction, accumulating in response to abiotic and biotic stress [43],[44]. Treatment with JA has been shown to induce cytosolic free-Ca<sup>2+</sup> concentration ([Ca<sup>2+</sup>] cyt) in *Arabidopsis thaliana* leaves [45]. However, high concentrations of JA inhibit cell expansion and cell wall modification and reduce plant growth [46],[47]. Thus downregulation of JA biosynthesis and signaling under drought stress in sedaxane treated plants is likely to act to establish new homeostasis through altered signaling and redirection of metabolism from defense/stress responses towards modification of plant growth and development.

#### 4.2.2.2 Cell Wall Modifications

Physical properties of the cell wall play a crucial role in the response of plants to drought [48]. Expansins mediate cell wall -loosening factors that directly induce turgor-driven cell wall extension [49]. Secondary wall-loosening enzymes such as xyloglucan endoglycosylase/hydrolases (XTHs) modify the structures of the cell wall, aiding cell wall loosening [50],[51]. Our microarray and qRT-PCR analyses showed upregulation of genes encoding cell-wall-loosening expansins and XTHs thus indicating that sedaxane is likely to confer adaptive responses to drought stress facilitating cellular expansion and modification of shoot growth and development. Upregulation of expansins genes have been implicated in increased drought tolerance in plants [42],[52].

#### 4.2.2.3 Tetrapyrrole biosynthesis

The tetrapyrrole biosynthetic pathway is responsible for the synthesis of different types of porphyrins in higher plants including chlorophyll and heme essential for several primary metabolic processes [53]. The major site of tetrapyrrole biosynthesis in plants occurs in plastids except the last steps of heme biosynthesis, which are possibly localized in both mitochondria and plastids [53]. In this study, expression of genes encoding various intermediates of the tetrapyrrole biosynthesis pathway was strongly upregulated in sedaxane treated plants suggesting that these plants were able to maintain a flux through the tetrapyrrole pathway under drought conditions. High level of tetrapyrrole intermediates has been

previously associated with improved drought tolerance in transgenic rice expressing *Myxococcus xanthus* protoporphyrinogen oxidase [54],[55]. Insertion of Mg<sup>2+</sup> into Protoporphyrin- IX by the enzyme Mg-chelatase was shown to favor the chlorophyll branch of the pathway [56]. In our data, genes encoding enzymes Magnesium-chelatase subunit and Mg-protoporphyrin IX, precursors for chlorophyll biosynthesis were upregulated. In plants, the protochlorophyllide reductase oxidoreductase (POR) step in tetrapyrrole pathway is strictly light-dependent, as it requires protochlorophyllide to be activated by light [57],[58]. In illuminated plants, protons are translocated from the stroma into the intra thylakoid lumen [59]. This movement is coupled with the release of Mg<sup>2+</sup>, into the stroma. These ion fluxes are known to contribute to an increase of the pH of the stroma from 7 to 8, an optimum pH of most enzymes involved in the Benson- Calvin cycle [60],[61], including rubisco, fructose-1,6-bisphosphatase, sedoheptulose-1,7-bisphosphatase, and phosphoribulokinase. Hence, the light-mediated increase of Mg<sup>2+</sup> and H<sup>+</sup> enhances the activity of key enzymes of the Calvin-Benson cycle. This coupled with the observed increased rate of photosynthesis would indicate a maintained balance between PSII activity and the Calvin cycle, thus protecting the PSII from photo damage.

Based on our results, the tetrapyrrole biosynthetic pathway is likely to be the target of sedaxane in wheat metabolism, driven by the production of glutamate in the mitochondria. Glutamate, the precursor for the synthesis of tetrapyrroles in plants is formed from 2-oxoglutarate and glutamine. 2-Oxoglutarate mainly produced in the mitochondria and transported to the chloroplast is an obligatory substrate for 2-oxoglutarate-dependent dioxygenases [62] and a key metabolite required for ammonia assimilation [63]. In this study, one of the upregulated top genes encode 2-oxoglutarate- dependent oxygenase. In addition, the tetrapyrrole intermediate Mg-protoporphyrin IX has been postulated to act as a signal molecule in signaling pathways between the chloroplast, nucleus and the mitochondria, and the accumulation of this metabolite is required to regulate the expression of genes encoding proteins associated with photosynthesis [64],[65].

### 4.3. Central Players in the Sedaxane Regulated Network

We aimed to identify a hub subnetwork to provide more insight on the physiological impact of sedaxane under drought conditions and ultimately to identify transcription factors that can potentially be used as candidate genes to improve photosynthetic performance of wheat. We used datasets from the leaves, roots and pregerminated seeds to identify 40 genes using inferred network stress and degree centralities, computed for each of the coexpressed regulatory genes in the network.

Our data suggest that dirigent proteins play a central role in protecting wheat plants against the effects of severe drought through their impact on mechanical strength and flexibility of cell wall. DIR-like family proteins have been implicated in cell wall lignin biosynthesis, which are structural cell wall components of vascular tissues [66]. The hub with the highest stress centrality in our network encoded the Hessian fly responsive protein 1 (HFR1), highly upregulated in the leaf and root, also considered a dirigent-like protein involved in modulating plant response to biotic stress [67] and previously implicated in cell wall strengthening via deposition of phenolics [68] and secretion of protective surface waxes [69].

Increased dry weight has been associated with accumulation of cell wall expansin [47]. One of the top ranked genes in the hub of the network encoded xyloglucan endotransglycosylase (XTH), involved in strengthening and cell wall plasticity leading to water uptake in leaves under drought conditions [51],[70]. The enrichment of pathways involved in cell wall modification, and upregulation of genes encoding XTHs and expansins in the leaf is an indication that, the selective loosening and strengthening of the cell wall in growing plant tissue under drought conditions is likely to stimulate water uptake to increase growth and development in the plant [71] which is consistent with increased dry weight in sedaxane treated plants under drought stress. A proline-rich protein precursor was also upregulated. Recent discoveries point out that proline is a key determinant of many cell wall proteins that plays important roles in plant growth and development. Interestingly, a gene encoding aquaporin, involved in regulating

water movement across cell membranes [72] was also upregulated in both leaf and root tissues. This suggests that water movement and use under drought conditions was enhanced with sedaxane treatment consistent with the physiological phenotype of increased photosynthesis and growth as well as reduction in NPQ of fungicide treated plants.

A gene hub encoding the calmodulin binding protein (CaM) was upregulated in both the leaf and pregerminated seeds. CaM is small  $\text{Ca}^{2+}$ -sensing protein that acts as signal transducer in a wide array of physiological processes including drought stress in plants [73],[74]. Using knockout mutants of the CaM transcription factors (CAMTAs), Pandey et al [75] showed that CaM was positively involved in drought stress tolerance in Arabidopsis. A new family of CaM-binding proteins, the type 1 non-specific lipid transfer proteins (nsLTPs) was identified in Arabidopsis [76]. In this study, we identified three hub genes encoding the nsLTPs, all upregulated in the leaf tissue. nsLTPs also act as wax transporters, able to transfer lipids and fatty acids across different membranes and are induced under drought stress [77]. nsLTPs have been shown to be involved in epicuticular wax or cuticle biosynthesis [78]. Kottapalli et al. [79] showed that epicuticular wax content increased in drought tolerant genotype of peanut (*Arachis hypogaea*). Loss of epicuticular wax has been associated with increased water loss in plants. In our study, one of the identified hub gene, the wax biosynthesis annotated as Ecriferum 1 (CER1) and WAX2-like protein (WAX2) was also upregulated.

Another interesting gene in the network which plays a regulatory role in signaling and abiotic stress tolerance is a transcriptional factor for glycine rich proteins (GRPs) [80]. The expression of GRP genes is modulated by plant hormones, which in turn regulate plant growth, development and stress responses [81]-[83]. In our study, GRP hub of genes was downregulated whereas GRPs have been shown to accumulate under drought [84].

#### **4.4. CONCLUSION**

This study showed that the SDHI sedaxane, applied as seed treatment, improved PSII efficiency, photosynthesis and biomass production of wheat under drought. These effects



were accompanied by low NPQ, as a result of a homeostasis between PSII activity and the Calvin cycle.

Transcriptomic analysis suggests that sedaxane enhances wheat seedling tolerance/resistance to drought stress by altering the expression of key genes/transcriptional factors from seed germination. We propose a schematic of the effects of sedaxane on plant physiology (Fig. 7) associated with differential patterns of nsLTPs, XTHs, CaM, HFR1, Zinc finger protein 1 known to regulate the expression of drought tolerance/resistance traits in crops. Initial responses were first observed in pregerminated seeds, where ROS scavenging genes were upregulated involved in the reduction of oxidative stress. In the root, defense-related genes were downregulated most likely to allow metabolites to be redirected towards adaptive development. The most differentially expressed genes were observed in leaves characterized by downregulation of jasmonate biosynthesis and signaling and increased chlorophyll biosynthesis allowing for the remobilization of assimilates from stress-related responses towards modified growth and development.

## **ACKNOWLEDGEMENTS**

This research was funded by Syngenta grant RK3537. We thank Dr Guillermina Mendiando for assistance with qRT-PCR.

## **Competing interests**

The authors declare that they have no competing interests.

598 **LITERATURE CITED**

- 599 [1] J.S. Boyer, Productivity and Environment, *Science* 218 (1982) 443–448. B
- 600 [2] N.R. Baker, Chlorophyll Fluorescence: A Probe of Photosynthesis In Vivo, *Annu.*  
601 *Rev. Plant Biol.* 59 (2008) 89–113.
- 602 [3] N.R. Baker, E. Rosenqvist, Applications of chlorophyll fluorescence can improve crop  
603 production strategies: an examination of future possibilities, *J. Exp. Bot.* 55 (2004)  
604 1607–1621. doi:10.1093/jxb/erh196.
- 605 [4] A.R. Reddy, K.V. Chaitanya, M. Vivekanandan, Drought-induced responses of  
606 photosynthesis and antioxidant metabolism in higher plants, *J. Plant Physiol.* 161  
607 (2004) 1189–1202. doi:10.1016/j.jplph.2004.01.013.
- 608 [5] M. Ashraf, P.J.C. Harris, Photosynthesis under stressful environments: An overview,  
609 *Photosynthetica* 51 (2013) 163–190.
- 610 [6] A.V. Ruban, M.P. Johnson, C.D.P. Duffy, The photoprotective molecular switch in the  
611 photosystem II antenna, *Biochim. Biophys. Acta - Bioenerg.* 1817 (2012) 167–181.  
612 doi:10.1016/j.bbabbio.2011.04.007.
- 613 [7] E.H. Murchie, K.K. Niyogi, Manipulation of photoprotection to improve plant  
614 photosynthesis, *Plant Physiol.* 155 (2011) 86–92. doi:10.1104/pp.110.168831.
- 615 [8] B. Demmig-Adams, W.W. Adams, U. Heber, S. Neimanis, K. Winter, A. Krüger, F.C.  
616 Czygan, W. Bilger, O. Björkman, Inhibition of zeaxanthin formation and of rapid  
617 changes in radiationless energy dissipation by dithiothreitol in spinach leaves and  
618 chloroplasts, *Plant Physiol.* 92 (1990) 293–301. doi:10.1104/pp.92.2.293.
- 619 [9] S. Hubbart, O.O. Ajigboye, P. Horton, E.H. Murchie, The photoprotective protein  
620 PsbS exerts control over CO<sub>2</sub> assimilation rate in fluctuating light in rice, *Plant J.* 71  
621 (2012) 402–412. doi:10.1111/j.1365-313X.2012.04995.x.
- 622 [10] Y. Fracheboud, J. Leipner, Practical applications of chlorophyll fluorescence in plant  
623 biology, in: J.R. DeEll, P.M.A. Toivonen (Eds.), Springer US, Boston, MA, 2003: pp.  
624 125–150. doi:10.1007/978-1-4615-0415-3\_4.

- 625 [11] O.O. Ajigboye, E. Murchie, R. V. Ray, Foliar application of isopyrazam and  
626 epoxiconazole improves photosystem II efficiency, biomass and yield in winter wheat,  
627 Pestic. Biochem. Physiol. 114 (2014) 52–60.
- 628 [12] C.A. Berdugo, U. Steiner, H.-W. Dehne, E.-C. Oerke Effect of bixafen on senescence  
629 and yield formation of wheat, Pestic. Biochem. Physiol. 104 (2012) 171–177.
- 630 [13] H.F. Avenot, T.J. Michailides, Progress in understanding molecular mechanisms and  
631 evolution of resistance to succinate dehydrogenase inhibiting (SDHI) fungicides in  
632 phytopathogenic fungi, Crop Prot. 29 (2010) 643–651.  
633 doi:10.1016/j.cropro.2010.02.019.
- 634 [14] R. Zeun, G. Scalliet, M. Oostendorp, Biological activity of sedaxane – a novel broad-  
635 spectrum fungicide for seed treatment, Pest Manag. Sci. 69 (2013) 527–534.  
636 doi:10.1002/ps.3405.
- 637 [15] X.G. Zhu, S.P. Long, D.R. Ort, Improving photosynthetic efficiency for greater yield.  
638 In S. Merchant, W.R. Briggs, and D. Ort, (eds), Annu. Rev. Plant Biol. 61 (2010) 235–  
639 261.
- 640 [16] R. Ren, X. Yang, R. V. Ray, Comparative aggressiveness of *Microdochium nivale*  
641 and *M. Majus* and evaluation of screening methods for *Fusarium* seedling blight  
642 resistance in wheat cultivars, Eur. J. Plant Pathol. 141 (2014) 281–294.
- 643 [17] C.J. Sturrock, J. Woodhall, M. Brown, C. Walker, S.J. Mooney, R. V Ray, Effects of  
644 damping-off caused by *Rhizoctonia solani* anastomosis group 2-1 on roots of wheat  
645 and oil seed rape quantified using X-ray Computed Tomography and real-time PCR,  
646 Front. Plant Sci. 6 (2015). doi:10.3389/fpls.2015.00461.
- 647 [18] R. Strasser, a Srivastava, M. Tsimilli-Michael, The fluorescence transient as a tool to  
648 characterize and screen photosynthetic samples, Probing Photosynthesis:  
649 Mechanism, Regulation & Adaptation (2000) 445–483.
- 650 [19] R.A. Irizarry, Exploration, normalization, and summaries of high density  
651 oligonucleotide array probe level data, Biostatistics 4 (2003) 249–264.

652 [20] O. Thimm, O. Blasing, Y. Gibon, A. Nagel, S. Meyer, P. Kruger, J. Selbig, L.A. Muller,  
653 S.Y. Rhee, M. Stitt, MAPMAN: a user-driven tool to display genomics data sets onto  
654 diagrams of metabolic pathways and other biological processes, *Plant J.* 37 (2004)  
655 914–939.

656 [21] Z. Du, X. Zhou, Y. Ling, Z. Zhang, Z. Su, AgriGO: a GO analysis toolkit for the  
657 agricultural community, *Nucleic Acids Res.* 38 (2010) 64–70.

658 [22] M.E. Smoot, K. Ono, J. Ruscheinski, P.L. Wang, T. Ideker, Cytoscape 2.8: new  
659 features for data integration and network visualization, *Bioinformatics* 27 (2011) 431–  
660 432

661 [23] A.R. Paolacci, O.A. Tanzarella, E. Porceddu, M. Ciaffi, Identification and validation of  
662 reference genes for quantitative RT-PCR normalization in wheat, *BMC Mol. Biol.* 10  
663 (2009) 1–27. doi:10.1186/1471-2199-10-11.

664 [24] C. Hutin, L. Nussaume, N. Moise, I. Moya, K. Kloppstech, M. Havaux, Early light-  
665 induced proteins protect Arabidopsis from photooxidative stress, *Proc. Natl. Acad.*  
666 *Sci. U. S. A.* 100 (2003) 4921–6. doi:10.1073/pnas.0736939100.

667 [25] W.J. Chen, T. Zhu, Networks of transcription factors with roles in environmental  
668 stress response, *Trends Plant Sci.* 9 (2004) 591–6.  
669 doi:10.1016/j.tplants.2004.10.007.

670 [26] H. Jeong, S.P. Mason, A.-L. Barabasi, Z.N. Oltvai, Lethality and centrality in protein  
671 networks, *Nature.* 411 (2001) 41–42.

672 [27] M.R.J. Carlson, B. Zhang, Z. Fang, P.S. Mischel, S. Horvath, S.F. Nelson, Gene  
673 connectivity, function, and sequence conservation: predictions from modular yeast  
674 co-expression networks, *BMC Genomics.* 7 (2006) 40. doi:10.1186/1471-2164-7-40.

675 [28] S. Dash, J. Van Hemert, L. Hong, R.P. Wise, J.A. Dickerson, PLEXdb: gene  
676 expression resources for plants and plant pathogens, *Nucleic Acids Res.* 40 (2012)  
677 D1194-201. doi:10.1093/nar/gkr938.

- 678 [29] N.R. Baker, A possible role for photosystem II in environmental perturbations of  
679 photosynthesis, *Physiol. Plant.* 81 (1991) 563–570. doi:10.1111/j.1399-  
680 3054.1991.tb05101.x.
- 681 [30] M. Brestic, G. Cornic, M.J. Freyer, N.R. Baker, Does photorespiration protect the  
682 photosynthetic apparatus in french bean leaves from photoinhibition during drought  
683 stress? *Planta* 196 (1995) 450–457. doi:10.1007/BF00203643.
- 684 [31] W.L. Araújo, A. Nunes-Nesi, S. Osorio, B. Usadel, D. Fuentes, R. Nagy, I. Balbo, M.  
685 Lehmann, C. Studart-Witkowski, T. Tohge, E. Martinoia, X. Jordana, F. M. DaMatta,  
686 A.R. Fernie, Antisense inhibition of the iron-sulphur subunit of succinate  
687 dehydrogenase enhances photosynthesis and growth in tomato via an organic acid–  
688 mediated effect on stomatal aperture, *Plant Cell* 23 (2011) 600–627.
- 689 [32] D. Fuentes, M. Meneses, A. Nunes-Nesi, W.L. Araújo, R. Tapia, I. Gómez, L.  
690 Holuigue, R.A. Gutiérrez, A.R. Fernie, X. Jordana A deficiency in the flavoprotein of  
691 Arabidopsis mitochondrial complex II results in elevated photosynthesis and better  
692 growth in nitrogen-limiting conditions, *Plant Physiol.* 157 (2011) 1114–1127.
- 693 [33] R.M. Acevedo , S.J. Maiale , S.C. Pessino , R. Bottini , O.A. Ruiz , P.A. Sansberro,  
694 A succinate dehydrogenase flavoprotein subunit-like transcript is upregulated in *Ilex*  
695 *paraguariensis* leaves in response to water deficit and abscisic acid, *Biochemistry* 65  
696 (2013) 48–54.
- 697 [34] K.A. Marrs, the functions and regulation of glutathione s-transferases in plants, *Annu.*  
698 *Rev. Plant Phys.* 47 (1996) 127–158.
- 699 [35] C.H. Foyer, G. Noctor, Redox homeostasis and antioxidant signaling: a metabolic  
700 interface between stress perception and physiological responses, *Plant Cell* 17  
701 (2005) 1866–1875
- 702 [36] R.N. Goodman, A.J. Novacky, The hypersensitive reaction in plants to pathogens. A  
703 resistance phenomenon, American Phytopathological Society Press St. Paul, MN  
704 (1994).

- 705 [37] L.C. Van Loon, Induced resistance in plants and the role of pathogenesis-related  
706 proteins. *Eur. J. Plant Pathol.* 103 (1997) 753–765
- 707 [38] P.J. Seo, M.J. Kim, J.-Y. Park, S.-Y. Kim, J. Jeon, Y.-H. Lee, J. Kim, C.-M. Park,  
708 Cold activation of a plasma membrane-tethered NAC transcription factor induces a  
709 pathogen resistance response in *Arabidopsis*, *Plant J.* 61 (2010) 661–671.
- 710 [39] A.G. Dobrikova, R.S. Vladkova, G.D. Rashkov, S.J. Todinova, S.B. Krumova, E.L.  
711 Apostolova, Effects of exogenous 24-epibrassinolide on the photosynthetic  
712 membranes under non-stress conditions., *Plant Physiol. Biochem.* 80 (2014) 75–82.  
713 doi:10.1016/j.plaphy.2014.03.022.
- 714 [40] T. Komatsu, H. Kawaide, C. Saito, A. Yamagami, S. Shimada, M. Nakazawa, M.  
715 Matsui, A. Nakano, M. Tsujimoto, M. Natsume, H. Abe, T. Asami, T. Nakano, The  
716 chloroplast protein BPG2 functions in brassinosteroid-mediated post-transcriptional  
717 accumulation of chloroplast rRNA., *Plant J.* 61 (2010) 409–422. doi:10.1111/j.1365-  
718 313X.2009.04077.x.
- 719 [41] R.M. Rivero, J. Gimeno, A. Van Deynze, H. Walia, E. Blumwald, Enhanced cytokinin  
720 synthesis in tobacco plants expressing PSARK::IPT prevents the degradation of  
721 photosynthetic protein complexes during drought, *Plant Cell Physiol.* 51 (2010)  
722 1929–1941. doi:10.1093/pcp/pcq143.
- 723 [42] A. Harb, A. Krishnan, M.M.R. Ambavaram, A. Pereira, Molecular and physiological  
724 analysis of drought stress in *Arabidopsis* reveals early responses leading to  
725 acclimation in plant growth, *Plant Physiol.* 154 (2010) 1254–1271.  
726 doi:10.1104/pp.110.161752.
- 727 [43] L. Li, C. Li, G.I. Lee, G. A. Howe, Distinct roles for jasmonate synthesis and action in  
728 the systemic wound response of tomato, *Proc. Natl. Acad. Sci. U. S. A.* 99 (2002)  
729 6416–6421. doi:10.1073/pnas.072072599.

730 [44] D.X. Xie, B.F. Feys, S. James, M. Nieto-Rostro, J.G. Turner, COI1: an Arabidopsis  
731 gene required for jasmonate-regulated defense and fertility, *Science* 280 (1998)  
732 1091–1094.

733 [45] J. Sun, V. Cardoza, D.M. Mitchell, L. Bright, G. Oldroyd, J.M. Harris, Crosstalk  
734 between jasmonic acid, ethylene and Nod factor signaling allows integration of  
735 diverse inputs for regulation of nodulation, *Plant J.* 46 (2006) 961–970.  
736 doi:10.1111/j.1365-313X.2006.02751.x.

737 [46] C. Ellis, I. Karafyllidis, C. Wasternack, J.G. Turner, The Arabidopsis mutant *cev1*  
738 links cell wall signaling to jasmonate and ethylene responses, *Plant Cell* 14 (2002)  
739 1557–1566.

740 [47] N. Onkokesung, I. Gális, C.C. von Dahl, K. Matsuoka, H.-P. Saluz, I.T. Baldwin,  
741 Jasmonic acid and ethylene modulate local responses to wounding and simulated  
742 herbivory in *Nicotiana attenuata* leaves, *Plant Physiol.* 153 (2010) 785–798.  
743 doi:10.1104/pp.110.156232.

744 [48] M.A. Bacon, The biochemical control of leaf expansion during drought. 101–112  
745 *Plant Growth Regul.* 29 (1999) 101–112.

746 [49] D.J. Cosgrove, Expansive growth of plant cell walls, *Plant Physiol. Biochem.* 38  
747 (2000) 109–124.

748 [50] D.J. Cosgrove, Loosening of plant cell walls by expansins, *Nature.* 407 (2000) 321–  
749 326. doi:10.1038/35030000.

750 [51] K. Swarup, E. Benková, R. Swarup, I. Casimiro, B. Péret, Y. Yang, G. Parry, E.  
751 Nielsen, I. De Smet, S. Vanneste, M.P. Levesque, D. Carrier, N. James, V. Calvo, K.  
752 Ljung, E. Kramer, R. Roberts, N. Graham, S. Marillonnet, K. Patel, J.D.G. Jones,  
753 C.G. Taylor, D.P. Schachtman, S. May, G. Sandberg, P. Benfey, J. Friml, I. Kerr, T.  
754 Beeckman, L. Laplaze, M.J. Bennett, The auxin influx carrier LAX3 promotes lateral  
755 root emergence, *Nat. Cell Biol.* 10 (2008) 946–954. doi:10.1038/ncb1754.

- 756 [52] D. Todaka, K. Shinozaki, K. Yamaguchi-Shinozaki, Recent advances in the  
757 dissection of drought-stress regulatory networks and strategies for development of  
758 drought-tolerant transgenic rice plants, *Front. Plant Sci.* 6 (2015) 84.  
759 doi:10.3389/fpls.2015.00084.
- 760 [53] R. Tanaka, A. Tanaka, Tetrapyrrole Biosynthesis in Higher Plants, *Annu. Rev. Plant*  
761 *Biol.* 58 (2007) 321–46. doi:10.1146/annurev.arplant.57.032905.105448.
- 762 [54] Y.B. Yun, J.I. Park, H.S. Choi, H. Jung, S.J. Jang, K. Back, Y.I. Kuk,  
763 Protoporphyrinogen oxidase-overexpressing transgenic rice is resistant to drought  
764 stress, *Crop Sci.* 53 (2013) 1076–1085.
- 765 [55] T.H. Phung, H. Jung, J.H. Park, J.G. Kim, K. Back, S. Jung, Porphyrin biosynthesis  
766 control under water stress: Sustained porphyrin status correlates with drought  
767 tolerance in transgenic rice, *Plant Physiol.* 157 (2011) 1746–1764.  
768 doi:10.1104/pp.111.188276.
- 769 [56] D.S.K. Nagahatenna, P. Langridge, R. Whitford, Tetrapyrrole-based drought stress  
770 signalling, *Plant Biotechnol. J.* 13 (2015) 447–459. doi:10.1111/pbi.12356.
- 771 [57] M. Gabruk, B. Mysliwa-Kurziel, Light-Dependent Protochlorophyllide  
772 Oxidoreductase: Phylogeny, Regulation, and Catalytic Properties, *Biochemistry.* 54  
773 (2015) 5255–5262. doi:10.1021/acs.biochem.5b00704.
- 774 [58] R.D. Willows, Biosynthesis of chlorophylls from protoporphyrin IX, *Nat. Prod. Rep.* 20  
775 (2015) 327–341
- 776 [59] G.H. Krause, movement of magnesium ions in intact chloroplasts, Spectroscopic  
777 determination with Eriochrome Blue SE, *BBA-Bioenergetics* 460 (1977) 500–510.
- 778 [60] W.H. Heldt, K. Werdan, M. Milovancev, G. Geller, Alkalization of the chloroplast  
779 stroma caused by light-dependent proton flux into the thylakoid space, *Biochim.*  
780 *Biophys. Acta.* 314 (1973) 224–241.



- 781 [61] K. Werdan, H.W. Heldt, M. Milovancev, The role of pH in the regulation of carbon  
782 fixation in the chloroplast stroma. Studies on CO<sub>2</sub> fixation in the light and dark,  
783 Biochim. Biophys. Acta. 396 (1975) 276–292.
- 784 [62] W.L. Araújo, A.O. Martins, A.R. Fernie, T. Tohge, 2-Oxoglutarate: linking TCA cycle  
785 function with amino acid, glucosinolate, flavonoid, alkaloid, and gibberellin  
786 biosynthesis, Front. Plant Sci. 5 (2014) 552. doi:10.3389/fpls.2014.00552.
- 787 [63] M. Hodges, Enzyme redundancy and the importance of 2-oxoglutarate in plant  
788 ammonium assimilation, J. Exp. Bot. 53 (2002) 905–916.
- 789 [64] A. Strand, T. Asami, J. Alonso, J.R. Ecker, J. Chory, Chloroplast to nucleus  
790 communication triggered by accumulation of Mg-protoporphyrinIX, Nature. 421  
791 (2003) 79–83. doi:10.1038/nature01204.
- 792 [65] Y. Kanesaki, Y. Kobayashi, M. Hanaoka, K. Tanaka, Mg-protoporphyrin IX signaling  
793 in Cyanidioschyzon merolae: multiple pathways may involve the retrograde signaling  
794 in plant cells, Plant Signal. Behav. 4 (2009) 1190–1192.
- 795 [66] L.B. Davin, N.G. Lewis, Dirigent proteins and dirigent sites explain the mystery of  
796 specificity of radical precursor coupling in lignan and lignin biosynthesis, Plant  
797 Physiol. 123 (2000) 453–462.
- 798 [67] S. Subramanyam, C. Zheng, J.T. Shukle, , CE, Williams, Hessian fly larval attack  
799 triggers elevated expression of disease resistance dirigent-like protein-encoding  
800 gene, HfrDrd, in resistant wheat, Arthropod Plant Interact. 7 (2013) 389–402.
- 801 [68] X. Liu, J. Bai, L. Huang, L. Zhu, X. Liu, N. Weng, J.C. Reese, M. Harris, J.J. Stuart,  
802 M.-S. Chen, Gene expression of different wheat genotypes during attack by virulent  
803 and avirulent hessian fly (*Mayetiola destructor*) Larvae, J. Chem. Ecol. 33 (2007)  
804 2171–2194. doi:10.1007/s10886-007-9382-2.
- 805 [69] D.K. Kosma, J.A. Nemacheck, M.A. Jenks, C.E. Williams, Changes in properties of  
806 wheat leaf cuticle during interactions with Hessian fly, Plant J. 63 (2010) 31–43.  
807 doi:10.1111/j.1365-313X.2010.04229.x.

- 808 [70] K. Vissenberg, M. Oyama, Y. Osato, R. Yokoyama, J.-P. Verbelen, K. Nishitani,  
809 Differential expression of AtXTH17, AtXTH18, AtXTH19 and AtXTH20 genes in  
810 Arabidopsis roots. Physiological roles in specification in cell wall construction, *Plant*  
811 *Cell Physiol.* 46 (2005) 192–200. doi:10.1093/pcp/pci013.
- 812 [71] D. J. Cosgrove, Plant cell wall extensibility: connecting plant cell growth with cell wall  
813 structure, mechanics, and the action of wall-modifying enzymes, *J. Exp. Bot.* 67  
814 (2015) 463–476.
- 815 [72] G. Li, V. Santoni, C. Maurel, Plant aquaporins: Roles in plant physiology, *Biochim.*  
816 *Biophys. Acta - Gen. Subj.* 1840 (2014) 1574–1582.  
817 doi:10.1016/j.bbagen.2013.11.004.
- 818 [73] W.A. Snedden, H. Fromm, Calmodulin, calmodulin-related proteins and plant  
819 responses to the environment, *Trends Plant Sci.* 3 (2016) 299–304.  
820 doi:10.1016/S1360-1385(98)01284-9.
- 821 [74] R.E. Zielinski, Calmodulin and calmodulin-binding proteins in plants, *Annu. Rev.*  
822 *Plant Physiol. Plant Mol. Biol.* 49 (1998) 697–725.
- 823 [75] N. Pandey, A. Ranjan, P. Pant, R. Tripathi, F. Ateek, H. Pandey, U. Patre, S. Sawant,  
824 CAMTA 1 regulates drought responses in *Arabidopsis thaliana*, *BMC Genomics.* 14  
825 (2013) 216. doi:10.1186/1471-2164-14-216.
- 826 [76] Z. Wang, W. Xie, F. Chi, C. Li, Identification of non-specific lipid transfer protein-1 as  
827 a calmodulin-binding protein in *Arabidopsis*, *FEBS Lett.* 579 (2005) 1683–1687.  
828 doi:10.1016/j.febslet.2005.02.024.
- 829 [77] F. Bourgis, J.-C. Kader, Lipid-transfer proteins: Tools for manipulating membrane  
830 lipids, *Physiol. Plant.* 100 (1997) 78–84. doi:10.1111/j.1399-3054.1997.tb03456.x.
- 831 [78] P. Sterk, H. Booij, G.A. Schellekens, A. Van Kammen, S.C. De Vries, Cell-specific  
832 expression of the carrot EP2 lipid transfer protein gene, *Plant Cell.* 3 (1991) 907–921.  
833 doi:10.1105/tpc.3.9.907.

- 834 [79] K.R. Kottapalli, R. Rakwal, J. Shibato, G. Burow, D. Tissue, J. Burke, N. Puppala, M.  
835 Burow, P. Payton, Physiology and proteomics of the water-deficit stress response in  
836 three contrasting peanut genotypes, *Plant. Cell Environ.* 32 (2009) 380–407.  
837 doi:10.1111/j.1365-3040.2009.01933.x.
- 838 [80] A.A. Rodríguez-Hernández, M.A. Ortega-Amaro, P. Delgado-Sánchez, J. Salinas,  
839 J.F. Jiménez-Bremont, AtGRDP1 gene encoding a glycine-rich domain protein is  
840 involved in germination and responds to aba signalling, *Plant Mol. Biol. Rep.* 32  
841 (2014) 1187–1202
- 842 [81] R. Long, Q. Yang, J. Kang, T. Zhang, H. Wang, M. Li, Z. Zhang, Overexpression of a  
843 novel salt stress-induced glycine-rich protein gene from alfalfa causes salt and ABA  
844 sensitivity in *Arabidopsis*, *Plant Cell Rep.* 32 (2013) 1289–1298. doi:10.1007/s00299-  
845 013-1443-0.
- 846 [82] C. Urbez, M. Cercós, M.A. Perez-Amador, J. Carbonell, Expression of PsGRP1, a  
847 novel glycine rich protein gene of *Pisum sativum*, is induced in developing fruit and  
848 seed and by ABA in pistil and root, *Planta.* 223 (2006) 1292–1302.  
849 doi:10.1007/s00425-005-0178-8.
- 850 [83] A.S. Reddy, B.W. Poovaiah, Accumulation of a glycine rich protein in auxin-deprived  
851 strawberry fruits, *Biochem. Biophys. Res. Commun.* 147 (1987) 885–891.
- 852 [84] J.A. Huerta-Ocampo, M.F. León-Galván, L.B. Ortega-Cruz, A. Barrera-Pacheco, A.  
853 De León-Rodríguez, G. Mendoza-Hernández, A.P.B. de la Rosa, Water stress  
854 induces up-regulation of DOF1 and MIF1 transcription factors and down-regulation of  
855 proteins involved in secondary metabolism in amaranth roots (*Amaranthus*  
856 *hypochondriacus* L.), *Plant Biol. (Stuttg).* 13 (2011) 472–482. doi:10.1111/j.1438-  
857 8677.2010.00391.x.

860 **TABLES**

861 **Table 1.** Biomass of wheat plants grown from sedaxane treated and untreated seeds 36  
862 days after germination. Each value is a mean (n=7) followed by standard error. SDX,  
863 sedaxane. UNT, untreated.  $AW_{FC}$ , available water at field capacity

864 **Table 2.** Mapman functional categories (BINs) in the cell function pathway for significantly  
865 up-and down-regulated genes ( $\geq 1.5$ -fold change;  $P < 0.05$ ) in (A) seeds after 48 h  
866 pregermination, and in (B) roots and (C) leaves of wheat plants grown from sedaxane  
867 treated and untreated seeds under drought stress (10%  $AW_{FC}$ ) 9 days after germination.

868 **Table 3.** Mapman functional categories in the metabolic pathways for significantly up-and  
869 down-regulated genes ( $\geq 1.5$ ) in leaves of wheat plants grown from sedaxane treated and  
870 untreated seeds under drought stress (10%  $AW_{FC}$ ) 9 days after germination.

871 **Table 4.** GO enrichment analysis for significantly up-and down-regulated genes ( $\geq 1.5$ -fold  
872 change;  $P < 0.05$ ) in seeds after 48 h pregermination. Analysis was performed using  
873 parametric analysis of gene set enrichment in AgriGO with Bonferroni multitest adjustment  
874 method. FC, fold change; FDR, false discovery rate; P, biological process; F, molecular  
875 function; C, cellular component. Red color system indicates upregulated and blue indicate  
876 downregulated terms.

877 **Table 5.** GO enrichment analysis for significantly up-and down-regulated genes ( $\geq 1.5$ -fold  
878 change;  $P < 0.05$ ) in leaves of wheat plants grown from sedaxane treated and untreated  
879 seeds under drought stress (10%  $AW_{FC}$ ) 9 days after germination. Analysis was performed  
880 using analysis of gene set enrichment in AgriGO with Bonferroni multitest adjustment  
881 method. FC, fold change; FDR, false discovery rate; P, biological process; F, molecular  
882 function; C, cellular component. Red color system indicates upregulated and blue indicate  
883 downregulated terms.

## FIGURES

**Fig. 1.** A, Efficiency of photosystem II (PSII) photochemistry ( $F_v'/F_m'$ ) in light adapted samples; B, Quantum yield (QY); C, Dissipated energy flux per active reaction center ( $Dlo/RC$ ), of leaves of wheat seedlings grown from sedaxane treated and untreated seeds. Error bars indicate mean  $\pm$  SE,  $n = 7$ . Asterisks indicate significant difference ( $P < 0.05$ ) from the untreated control. SDX, Sedaxane, UNT, Untreated.

**Fig. 2.** Light response of photochemical quenching (qP) of drought-stressed (10%  $AW_{FC}$ ) and non-stressed (90%  $AW_{FC}$ ) plants 12 days after germination. Error bars indicate mean  $\pm$  SE,  $n = 7$ . Asterisks show a significant difference ( $P < 0.05$ ) from the untreated control.  $AW_{FC}$  - available water at field capacity.

**Fig. 3.** Light response of A, dissipated excess excitation energy measured as non-photochemical quenching (NPQ) and B, rate of  $CO_2$  assimilation ( $A$ ) in leaves of wheat plants grown from sedaxane treated and untreated seeds 12 DAG. Error bars indicate mean  $\pm$  SE,  $n = 7$ . Asterisks in A, indicate differences ( $P < 0.05$ ) from the untreated control. In B, asterisks indicate significant interaction ( $P < 0.05$ ) between fungicide sedaxane and available water at field capacity ( $AW_{FC}$ ). SDX, sedaxane. UNT, Untreated.

**Fig. 4.** Venn diagram comparing up-regulated genes (adjusted  $P < 0.05$ ; Fold change  $\geq 1.5$ ) in leaf and root tissues of plants grown from sedaxane treated seeds and treated seed after 48hr pregermination.

**Fig. 5.** Coexpression and regulatory interaction network of common top differentially expressed genes across the tissues (leaf, root and pregerminated seeds). The subnetwork was implemented and visualized in Cytoscape. Nodes were coloured based on stress degree, red, brown and yellow represented highest, high and middle stress respectively. The edge colour and thickness represent the degree of co-expressed connections from strong (thick and brown) to weak (thin and green).

**Fig. 6.** Expression levels of candidate genes by microarray and qRT-PCR. Genes were selected from gene network analysis across leaf, root and pregerminated tissues. The array and qRT-PCR data are averages of 3 biological replicates of minimum of 3 plants each. Error bars indicate mean  $\pm$  SE. Asterisks show significant differences in candidate gene expression levels compared to the corresponding control (\* $P < 0.05$ ). NE: new experiment.

**Fig. 7.** Molecular responses to sedaxane in individual plant tissues and across tissues and their effect on plant physiology. Sedaxane induced transcriptional regulation of genes and transcriptional factors resulting in protection against oxidative stress in pregerminated seeds, downregulation of pathogenesis related genes at 9 days after germination under drought conditions in the root tissues; coupled with altered hormone signaling and metabolism in the leaves to mobilize metabolites towards growth and adaptive development leading to increased drought tolerance with improved photosynthesis and growth.

922 **Appendix A. Supplementary data**

923 **Fig. S1.** Light response of plants drought-stressed (10%  $AW_{FC}$ ) and non-stressed (90%  
924  $AW_{FC}$ ) plants 12 days after germination. A, Stomatal conductance. B, Transpiration rates.  
925 Error bars indicate mean  $\pm$  SE, n = 7. Asterisks show a significant difference ( $P < 0.05$ ) from  
926 the untreated control.  $AW_{FC}$  - available water at field capacity.

927 **Table S1.** List of targeted genes for qRT-PCR.

928 **Table S4.** Functional categories in the MapMan 'metabolism overview' of differentially  
929 regulated genes (adjusted  $P < 0.05$ ) in the leaf of drought stressed wheat plants grown from  
930 sedaxane treated seeds.

931 **Table S5.** Centralities based analysis and the values of the top 40 ranked genes

932 **Appendix B. Supplementary data**

933 **Table S2.**

934 **A.** Differentially regulated transcripts (adjusted  $P < 0.05$ ) in sedaxane treated- pregerminated  
935 seeds

936 **B.** Differentially regulated transcripts (adjusted  $P < 0.05$ ) in the root of drought stressed wheat  
937 plants grown from sedaxane treated seeds

938 **C.** Differentially regulated transcripts (adjusted  $P < 0.05$ ) in the leaf of drought stressed wheat  
939 plants grown from sedaxane treated seeds

940 **Appendix C. Supplementary data**

941 **Table S3.**

942 **A.** Functional categories in the Mapman 'cell function overview' of differentially regulated  
943 genes (adjusted  $P < 0.05$ ) in sedaxane treated pregerminated seeds

944 **B.** Functional categories in the MapMan 'cell function overview' of differentially regulated  
945 genes (adjusted  $P < 0.05$ ) in the root of drought stressed wheat plants grown from sedaxane  
946 treated seeds.

947 **C.** Functional categories in the MapMan 'cell function overview' of differentially regulated  
948 genes (adjusted  $P < 0.05$ ) in the leaf of drought stressed wheat plants grown from sedaxane  
949 treated seeds.

950

951



1 **TABLE 1.**

2 Biomass of wheat plants grown from sedaxane treated and untreated seeds 36 days after germination.

Fungicide	Tiller no.		Height (cm)		Water content (%)		Dry weight (g)	
	10% AW <sub>FC</sub>	90% AW <sub>FC</sub>	10% AW <sub>FC</sub>	90% AW <sub>FC</sub>	10% AW <sub>FC</sub>	90% AW <sub>FC</sub>	10% AW <sub>FC</sub>	90% AW <sub>FC</sub>
SDX	8 ± 1	35 ± 2	18.31 ± 0.23	36.05 ± 0.48	73.51 ± 2.77	86.68 ± 0.51	0.27 ± 0.03	0.13 ± 0.01
UNT	7 ± 1	33 ± 2	17.03 ± 0.51	36.71 ± 0.52	83.12 ± 1.1	88.4 ± 0.95	0.17 ± 0.01	0.12 ± 0.01
Effects	P	LSD	P	LSD	P	LSD	P	LSD
Fungicide	0.432	3.176	0.478	0.955	0.003	3.438	0.003	0.035
AW <sub>FC</sub>	<0.001	3.176	<0.001	0.955	<0.001	3.438	<0.001	0.035
Fungicide x AW <sub>FC</sub>	0.547	4.491	0.044	1.351	0.027	4.862	0.027	0.049

3 Each value is a mean (n=7) followed by standard error. SDX, sedaxane. UNT, untreated. AW<sub>FC</sub>, available water at field capacity. Dry weight is  
 4 expressed relative to fresh weight

5

**TABLE 2.**

Mapman functional categories (BINs) in the cell function pathway for significantly up-and down-regulated genes ( $\geq 1.5$  fold change;  $P < 0.05$ ) in (A) seeds after 48 hrs pregermination, and in (B) roots and (C) leaves of wheat plants grown from sedaxane treated and untreated seeds under drought stress (10%  $AW_{FC}$ ) 9 days after germination.

	Bin	Name	Up	Down	P Value
A. Pregerminated seeds	28.1	DNA.synthesis/Chromatin structure.histone	2	84	3.67E-12
	20.1	Stress.biotic	3	18	2.30E-02
	35.2	Not assigned/unknown	355	750	1.10E-02
B. Roots	20.1	Stress. biotic	0	10	2.00E-02
C. Leaves	29.2	Protein synthesis	58	16	6.56E-13
	17	Hormone metabolism	5	47	2.20E-07
	20.1	Stress.biotic	4	29	3.84E-05
	29.4	Protein.postranslational	7	35	5.40E-02
	30	Signalling	13	53	5.40E-02
	26	Misc	65	54	5.40E-02

$AW_{FC}$ , available water at field capacity

**TABLE 3.**

Mapman functional categories in the metabolic pathway for significantly up-and down-regulated genes ( $\geq 1.5$ ) in leaves of wheat plants grown from sedaxane treated and untreated seeds under drought stress (10%  $AW_{FC}$ ) 9 days after germination.

Bin	Name	Up	Down	<i>P</i> value
10.7	Cell wall.modification	12	1	2.64E-06
19	Tetrapyrrole synthesis	8	0	4.00E-02

$AW_{FC}$ , available water at field capacity

**TABLE 4.**

GO enrichment analysis of pathways for significantly up-and down-regulated genes ( $\geq 1.5$  fold change;  $P < 0.05$ ) in seeds after 48 h pregermination.

GO Term	Ontology Source	Description	No. Input List	Mean Log <sub>2</sub> FC	Z-score	FDR
GO:0006575	P	cellular amino acid derivative metabolic process	20	0.28	3.3	8.70E-03
GO:0006790	P	sulfur metabolic process	16	0.37	3.3	8.70E-03
GO:0006803	P	glutathione conjugation reaction	10	0.59	3.3	8.70E-03
GO:0006749	P	glutathione metabolic process	10	0.59	3.3	8.70E-03
GO:0006518	P	peptide metabolic process	10	0.59	3.3	8.70E-03
GO:0051186	P	cofactor metabolic process	18	0.26	3.1	1.40E-02
GO:0009057	P	macromolecule catabolic process	13	0.36	3	2.00E-02
GO:0006732	P	coenzyme metabolic process	15	0.27	2.8	2.80E-02
GO:0006091	P	generation of precursor metabolites and energy	19	0.17	2.8	3.30E-02
GO:0009056	P	catabolic process	22	0.09	2.6	4.70E-02
GO:0051707	P	response to other organism	18	-1.2	-2.6	4.70E-02
GO:0009607	P	response to biotic stimulus	23	-1.1	-2.7	4.60E-02
GO:0044085	P	cellular component biogenesis	40	-1	-3.1	1.40E-02
GO:0065003	P	macromolecular complex assembly	35	-1.1	-3.3	8.70E-03
GO:0043933	P	macromolecular complex subunit organization	35	-1.1	-3.3	8.70E-03
GO:0034622	P	cellular macromolecular complex assembly	35	-1.1	-3.3	8.70E-03
GO:0034621	P	cellular macromolecular complex subunit organization	35	-1.1	-3.3	8.70E-03
GO:0022607	P	cellular component assembly	35	-1.1	-3.3	8.70E-03
GO:0016043	P	cellular component organization	50	-1	-3.5	6.90E-03
GO:0051276	P	chromosome organization	36	-1.2	-3.7	3.90E-03
GO:0006996	P	organelle organization	42	-1.1	-3.7	3.90E-03
GO:0065004	P	protein-DNA complex assembly	29	-1.3	-3.8	2.90E-03
GO:0034728	P	nucleosome organization	29	-1.3	-3.8	2.90E-03
GO:0031497	P	chromatin assembly	29	-1.3	-3.8	2.90E-03
GO:0006334	P	nucleosome assembly	29	-1.3	-3.8	2.90E-03
GO:0006323	P	DNA packaging	30	-1.2	-3.8	2.90E-03
GO:0006333	P	chromatin assembly or disassembly	31	-1.3	-4	2.90E-03
GO:0006325	P	chromatin organization	33	-1.2	-4	2.90E-03
GO:0071103	P	DNA conformation change	31	-1.3	-4	2.90E-03
GO:0004364	F	glutathione transferase activity	12	0.74	4.1	4.20E-03
GO:0048037	F	cofactor binding	32	0.15	3.5	1.30E-02
GO:0016765	F	transferase activity, transferring alkyl or aryl (other than methyl) groups	14	0.46	3.4	1.40E-02
GO:0003676	F	nucleic acid binding	96	-0.85	-3.2	2.50E-02
GO:0003677	F	DNA binding	79	-0.93	-3.5	1.30E-02

Analysis was performed using parametric analysis of gene set enrichment in AgriGO with Bonferroni multitest adjustment method. FC, fold change; FDR, false discovery rate; P, biological process; F, molecular function; C, cellular component. Red color system indicates upregulated and blue indicate downregulated terms

1 **TABLE 5.**

2 GO enrichment analysis of pathways for significantly up-and down-regulated genes ( $\geq 1.5$  fold change;  $P < 0.05$ ) in  
3 leaves of wheat plants grown from sedaxane treated and untreated seeds under drought stress (10%  $AW_{FC}$ ) 9 days  
4 after germination.

GO Term	Ontology Source	Description	No. Input List	Mean $\log_2FC$	Z-score	FDR
GO:0006412	P	translation	56	0.56	6.3	5.10E-08
GO:0042254	P	ribosome biogenesis	41	0.59	5.6	2.00E-06
GO:0022613	P	ribonucleoprotein complex biogenesis	42	0.56	5.5	3.10E-06
GO:0044085	P	cellular component biogenesis	57	0.34	4.5	2.00E-04
GO:0009059	P	macromolecule biosynthetic process	123	0.15	4.1	9.30E-04
GO:0034645	P	cellular macromolecule biosynthetic process	109	0.12	3.5	8.50E-03
GO:0044249	P	cellular biosynthetic process	208	0.04	3.4	8.50E-03
GO:0033013	P	tetrapyrrole metabolic process	11	0.72	3.4	8.50E-03
GO:0015994	P	chlorophyll metabolic process	11	0.72	3.4	8.50E-03
GO:0006778	P	porphyrin metabolic process	11	0.72	3.4	8.50E-03
GO:0009058	P	biosynthetic process	220	0.03	3.4	9.60E-03
GO:0010467	P	gene expression	108	0.09	3.1	2.50E-02
GO:0009309	P	amine biosynthetic process	11	0.58	2.9	3.90E-02
GO:0008652	P	cellular amino acid biosynthetic process	11	0.58	2.9	3.90E-02
GO:0044267	P	cellular protein metabolic process	146	0.03	2.8	4.60E-02
GO:0009607	P	response to biotic stimulus	26	-0.64	-2.8	4.60E-02
GO:0051707	P	response to other organism	24	-0.69	-3	3.30E-02
GO:0051704	P	multi-organism process	24	-0.69	-3	3.30E-02
GO:0006952	P	defense response	31	-0.74	-3.7	4.50E-03
GO:0009695	P	jasmonic acid biosynthetic process	11	-1.3	-4.5	2.00E-04
GO:0009694	P	jasmonic acid metabolic process	11	-1.3	-4.5	2.00E-04
GO:0031408	P	oxylipin biosynthetic process	20	-1	-4.5	2.00E-04
GO:0031407	P	oxylipin metabolic process	20	-1	-4.5	2.00E-04
GO:0003735	F	structural constituent of ribosome	61	0.57	6.7	1.40E-09
GO:0005198	F	structural molecule activity	66	0.54	6.7	1.40E-09
GO:0019843	F	rRNA binding	17	0.97	5.4	1.60E-06
GO:0003723	F	RNA binding	42	0.50	5	6.30E-06
GO:0016757	F	transferase activity, transferring glycosyl groups	32	0.32	3.2	1.20E-02
GO:0016758	F	transferase activity, transferring hexosyl groups	24	0.35	2.9	2.90E-02
GO:0032561	F	guanyl ribonucleotide binding	11	0.55	2.8	3.60E-02
GO:0019001	F	guanyl nucleotide binding	11	0.55	2.8	3.60E-02
GO:0005525	F	GTP binding	11	0.55	2.8	3.60E-02
GO:0048037	F	cofactor binding	32	-0.58	-2.7	4.40E-02
GO:0050662	F	coenzyme binding	25	-0.65	-2.8	3.60E-02
GO:0004674	F	protein serine/threonine kinase activity	44	-0.78	-4.7	2.40E-05
GO:0004672	F	protein kinase activity	58	-0.74	-5.1	5.70E-06
GO:0016772	F	transferase activity, transferring phosphorus-containing groups	97	-0.61	-5.1	5.70E-06
GO:0016773	F	phosphotransferase activity, alcohol group as acceptor	64	-0.74	-5.3	2.70E-06
GO:0016301	F	kinase activity	83	-0.67	-5.3	2.50E-06

5 Analysis was performed using analysis of gene set enrichment in AgriGO with Bonferroni multitest adjustment method.  
6 FC, fold change; FDR, false discovery rate; P, biological process; F, molecular function; C, cellular component. Red  
7 color system indicates upregulated and blue indicate downregulated terms.  $AW_{FC}$ , available water at field capacity

**Fig. 1**

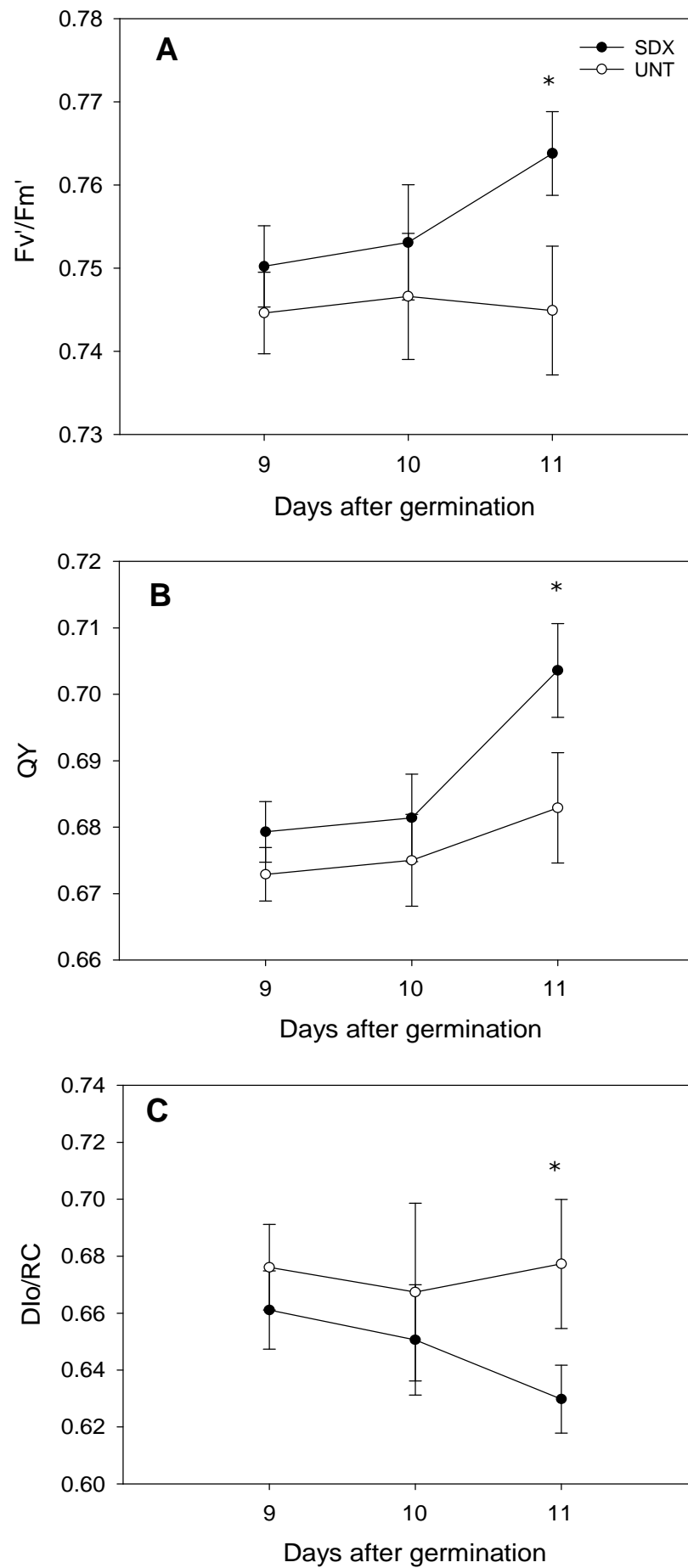


Fig. 2.

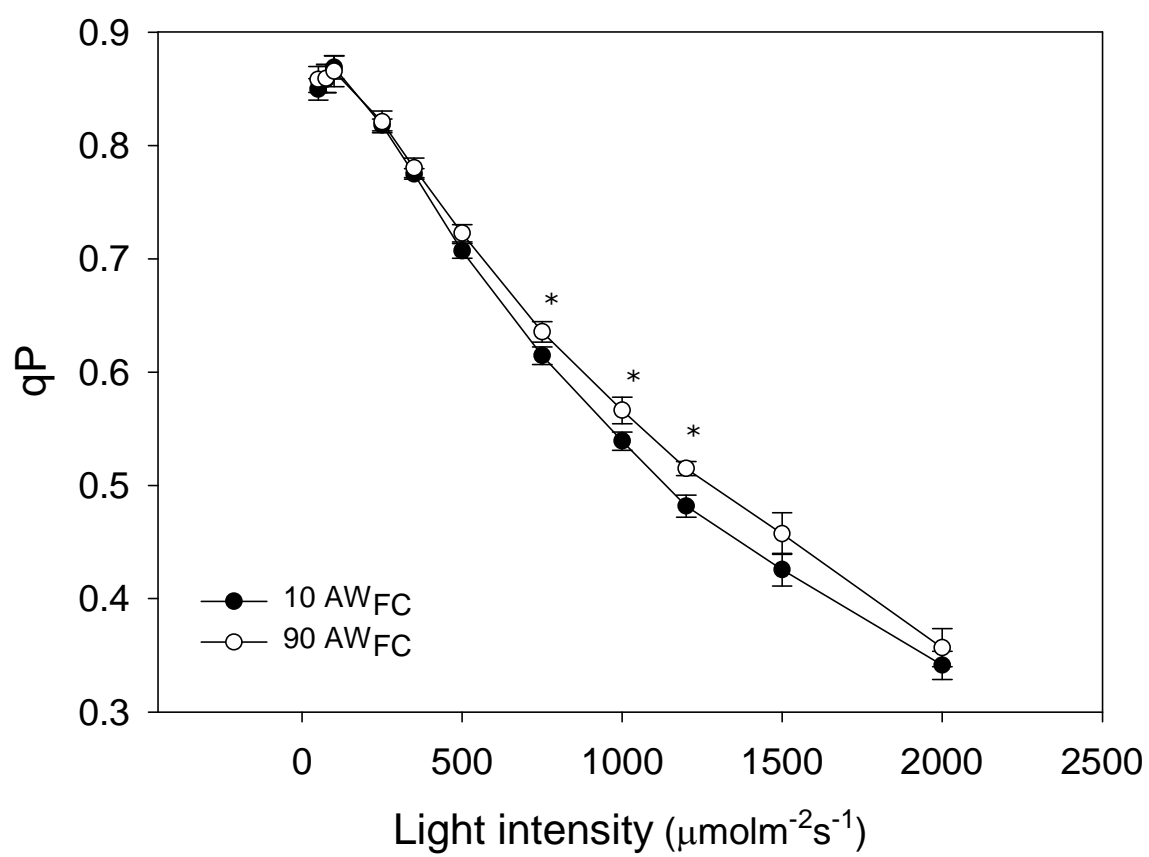


Fig. 3.

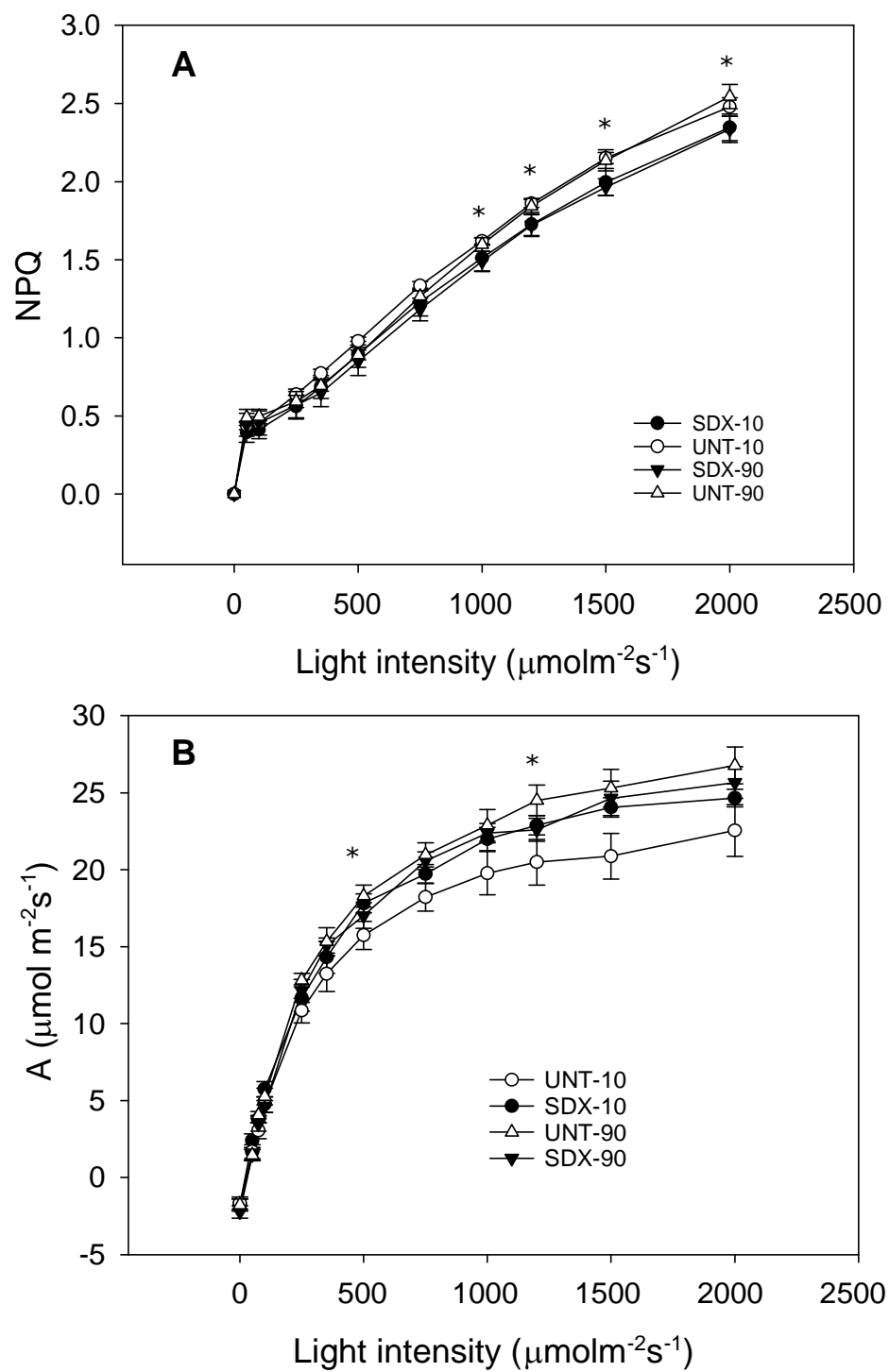




Fig. 4.

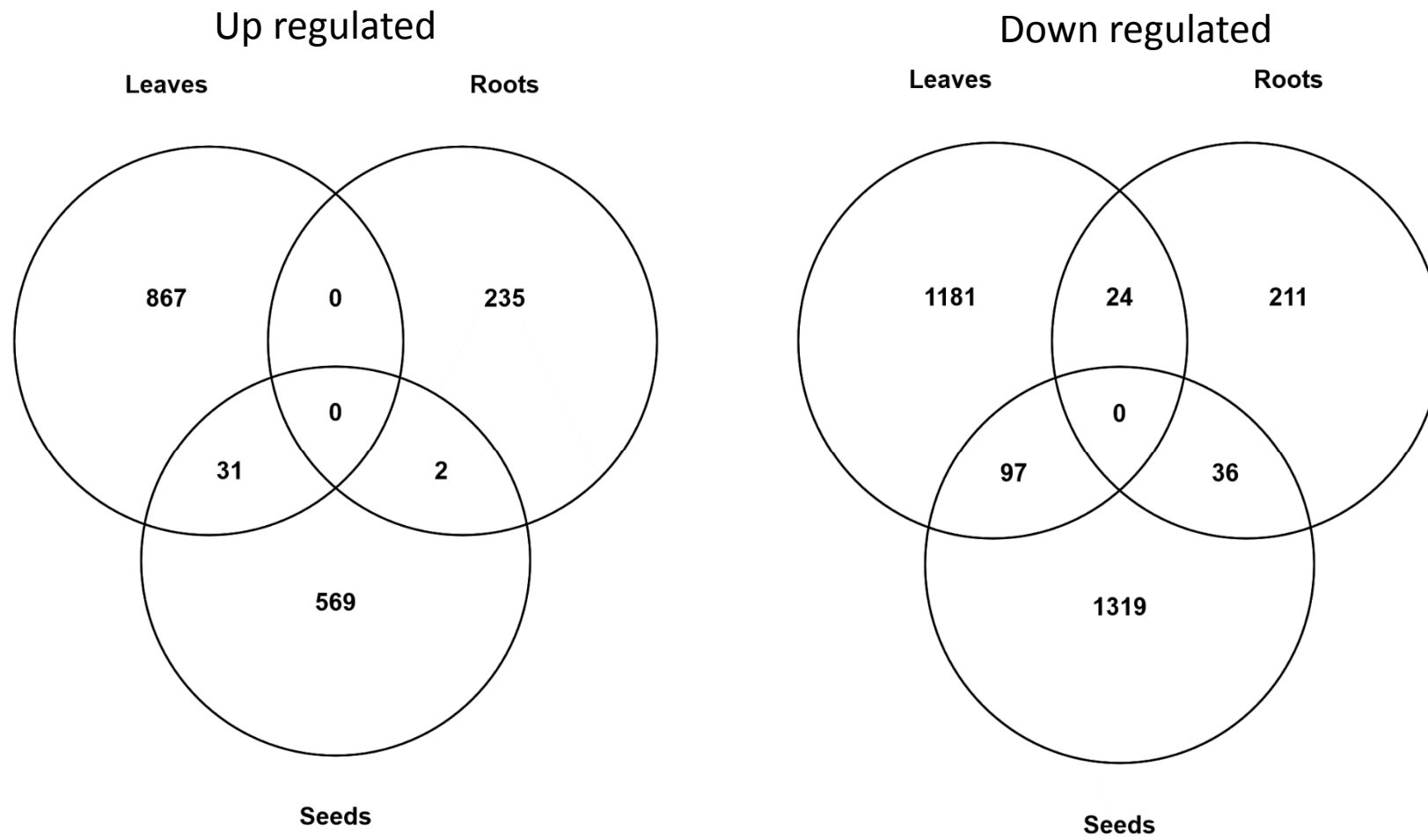


Fig. 5.

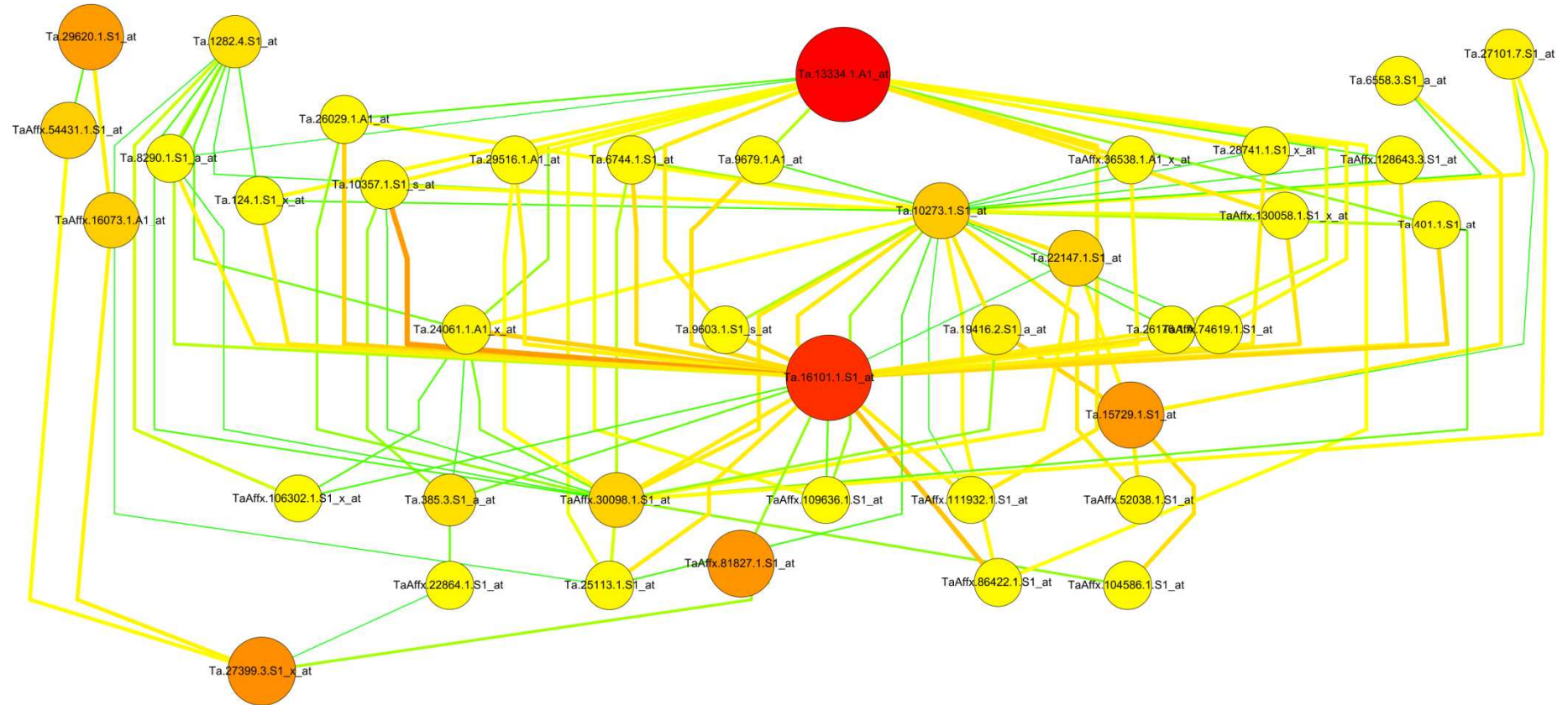
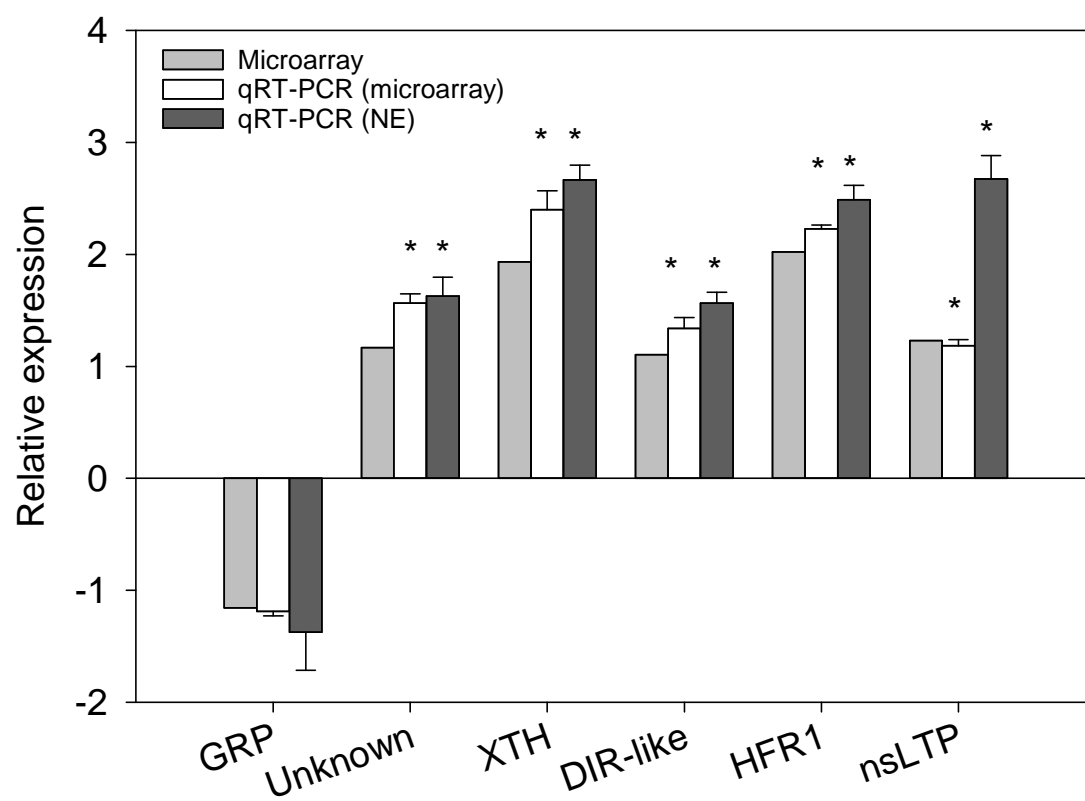


Fig. 6.



**Fig. 7.**

